Analysis of Electromagnetic and Seismic Geophysical Methods for Investigating Shallow Sub-surface Hydrogeology

Eric M. Parks

A thesis submitted to the faculty of

Brigham Young University

in partial fulfillment of the requirements for the degree of

Masters of Science

Stephen T. Nelson, Chair

John H. McBride

Alan L. Mayo

Department of Geological Sciences

Brigham Young University

April 2010

ABSTRACT

Analysis of Electromagnetic and Seismic Geophysical Methods for

Investigating Shallow Sub-surface Hydrogeology

Eric M. Parks

Department of Geological Sciences

Master of Science

An integrated electromagnetic (EM) and seismic geophysical study was performed to evaluate non-invasive approaches to estimate depth to shallow groundwater in arid environments with elevated soil salinity where the installation of piezometers would be impractical or prohibited. Both methods were tested in two study areas (semi-arid and arid respectively), one in Palmyra, Utah, USA near the shore of Utah Lake where groundwater is shallow and unconfined in relatively homogeneous lacustrine sediments. The other area is Carson Slough, Nevada, USA near Ash Meadows National Wildlife Refuge in Amargosa Valley. The area is underlain by valley fill, with generally variable shallow depths to water in an ephemeral braided stream environment. The methods used include frequency domain electromagnetic induction allowing for multiple antenna-receiver spacings. High resolution compressional P-wave seismic profiles using a short (0.305 m) geophone spacing for common depth-point reflection stacking and first arrival modeling were also acquired. Both methods were deployed over several profiles where shallow piezometer control was present. The semi-arid Palmyra site with its simpler geohydrology serves as an independent calibration to be compared to the Carson Slough Site.

EM results at both sites show that water surfaces correspond with a drop in conductivity. This is due to elevated concentrations of evaporative salts in the vadose zone immediately above the water table. EM and seismic profiles at the Palmyra site were readily correlated to depth to groundwater in monitoring wells demonstrating that the method is ideal under laterally homogeneous conditions. Interpreting the EM and seismic profiles at Carson Slough was challenging due to the laterally and vertically variable soil types, segmented perched water surfaces, and strong salinity variations.

The high-resolution images and models provided by the seismic profiles confirm the simple soil and hydrological structure at the Palmyra site as well as the laterally complex structure at Carson Slough. The EM and seismic results indicate that an integrated geophysical approach is necessary for an area like Carson Slough, where continued leaching of salts combined with braided stream deposition has created a geophysically complex soil and groundwater system.

ACKNOWELDGEMENTS

There are many people that I have reason to be grateful to for helping me reach my goal of graduating with a master's degree. I cannot name them all here, but I would first like to thank Dr. Steve Nelson, Dr. John McBride, Dr. Alan Mayo, and Prof. David Tingey for their help from the beginning stages of this thesis project. Thank you each for always being available to help me with my questions, both in coursework and my thesis research. I would also like to thank all the professors and student assistants who helped me with field work in summer heat of the Amargosa Desert and along the shore of Utah Lake.

I gratefully acknowledge software grants to Brigham Young University from the Landmark (Halliburton) University Grant Program (ProMAX2D™) and from Seismic Micro-Technology (The Kingdom Suite™). Partial funding for this project was provided by Nye County (Nevada) Department of Natural Resources and by the College of Physical and Mathematical Sciences, Brigham Young University. I would also like to thank the Nature Conservancy for allowing me allowing me to use their property in Palmyra, Utah for a portion of this study.

Lastly I would like to thank my family for their support. I would like to thank my parents who have always encouraged me to explore, to learn, and to reach for my goals. Finally, I want to thank my wife Sarah for her support all along my journey as a graduate student. She has helped me in the field, in the lab, at home, and at conferences.

TABLE OF CONTENTS

LIST OF TABLES

LIST OF FIGURES

INTRODUCTION

Characterization of water resources in arid environments that face human development is critical. Desert regions often have abundant biological diversity, as well as many endangered or threatened species, which depend on these shallow water systems. The Amargosa Desert is one of the driest regions in the western USA and several species there are facing pressure from modern human development and urban expansion (Anderson, 2005; Hasselquist and Allen, 2009; Johnston and Zink, 2003; Sada, 1990). Better constraints on understanding shallow (<5 m) groundwater in this type of region could be determined by drilling or trenching; however, this is often impractical, prohibitively expensive, or, in protected habitats, generally prohibited. For these reasons, there are many desert areas where a non-invasive approach to mapping shallow groundwater could be very valuable. Geophysical tools may be of use to provide the needed data to estimate depth to water. However, the use of classical geophysical methods (e.g., seismic refraction and electrical resistivity) to measure depth to shallow ground water (< 5 m) in areas with high soil and water salinity and complex shallow geology presents many challenges. This study is meant to determine the effectiveness and feasibility of frequency domain electromagnetic (FEM) conductivity measurements and shallow high-resolution seismic methods to determine depth to and lateral structure of shallow groundwater in arid regions with elevated soil salinity, and complex near-surface geology. Seismic profiles were collected to provide a calibration and comparison to FEM measurements.

Understanding depth to shallow groundwater in arid regions is critical for accurate estimation of water loss due to evapotranspiration (ET). Carson Slough is one such area where water resources are facing increased pressure by human development. Its location, adjacent to Ash Meadows Wildlife Refuge, with several endangered species of plants and animals (Sada, 1990), and proximity to growing cities like Pahrump, Nevada, which has shown continued population growth and a net decrease in water levels of up to 18.3 m in the valley fill aquifer due to pumping (Harrill, 1986; Stonestrom et al., 2007), makes it a good location for this geophysical study. Greater accuracy in depth to water estimates could contribute to better ET estimates which will improve the water budget resulting in more sustainable use of water in the area.

Study Areas

In order to provide a simple control on the interpretation of geophysical data from the arid site, two study areas were selected. The first is 450 m from the southern shore of Utah Lake, in Palmyra, Utah near the Provo Bay outlet (Figure 1-A). The second is at Carson Slough, Nevada south of Ash Meadows National Wildlife Reserve (AMNWR) in the Amargosa Desert located about 115 km northwest of Las Vegas, Nevada (Figure 1-B). The majority of soil samples from both study areas indicate that the soils would be classified as saline soils, defined by an electrical conductivity (EC) of the saturation extract >4 dS/m (400mS/m), although many scientists are urging that the minimum EC for saline soils be defined as >2dS/m (400 mS/m) (Rhoades, 1993; Sparks, 2003).

The Utah Lake site was chosen because it is similar to Carson Slough in being semi-arid and with elevated salinity and shallow water, but less sedimentologically and hydrogeologically complex, allowing for comparison of the data and evaluation of the methodology in two different ranges of complexity.

The site at Carson Slough was chosen for its proximity to AMNWR, a protected area where water levels are shallow, not well defined, and a non-invasive approach to determine depth to groundwater would be greatly beneficial.

Local Geologic and Hydrogeologic Settings

The Palmyra site is located in southern Utah Valley, which is part of the Utah Lake watershed of the Great Salt Lake Basin (Figure 1). Utah Valley formed as a result of Tertiary Basin and Range extension and corresponds to the boundary between the Basin and Range and Rocky Mountain Provinces (Clark and Apple, 1985). The shallow valley subsurface is composed mainly of Quaternary fluvial sediments and Pleistocene Lake Bonneville sediments and inter-fingered alluvial fan deposits (Bissel, 1963; Sanderson, 2002). Surface sediments at the Palmyra site have been mapped as sand and silty alluvium, upper Pleistocene to Holocene in age (Bissel, 1963).

Four significant groundwater systems have been identified within Utah Valley and the bounding Wasatch mountains, (Barnhurst, 2003); however, only the upper portion of the shallow alluvial groundwater system is of interest to this particular investigation. Sediments in this generally unconfined aquifer are granular sediments with only sparse and thin confining units (Utah Division of Water Resources, 1997). Water levels in this area range from about 1.5 m below ground surface near the lake to about 120 m near the Wasatch Mountain front to the east (Sanderson, 2002). Because the location of investigation is so close to the lake, the water table varies only with fluctuations in lake level. The average precipitation for the area is 52.5 cm/yr (Sanderson, 2002).

The Carson Slough site is located in the Amargosa Desert, which is part of the Death Valley watershed in southwestern Nevada and southeastern California (Figure 1). It has a surface drainage area of about 6700 km^2 (Walker and Eakin, 1963) and ranges in elevation from 670 m to 2100 m with corresponding mean annual precipitation ranging from 5 cm to 38 cm (Classen, 1985). The Amargosa basin is bounded by northwest-trending mountain ranges of

Precambrian quartzite and Paleozoic quartzite and dolomite (Sweetkind et al., 2001). The basin formed as a result of middle to late Cenozoic Basin and Range extension (Grose and Smith, 1989). Valley fill, which reaches thicknesses of up to 550 m (Winograd and Thordarson, 1975), is composed of alluvial fans, playas, eolian, lacustrine, fluvial, and spring deposits (Workman et al., 2001). Kilroy (1991) classified and described the valley fill sediments into five lithologies as follows: moderately sorted river-channel sediments from clay to gravel size, poorly to well-sorted, fine-grained playa sediments, poorly-sorted silt to gravel sized alluvial fan sediments, fine-grained vuggy freshwater limestones, and moderately indurated Tertiary conglomerates. Winograd and Thordarson (1975) remarked that the valley fill is generally poorly stratified and poorly sorted and that strata are horizontal but usually discontinuous. They also noted that caliche is a cementing agent found at almost all depths. The valley fill is underlain by lava flows, tuffs, and Paleozoic carbonates, sandstones, mudstones, and conglomerates (Workman et al., 2001).

Four main hydrogeologic units exist in the Amargosa Basin. These have been identified by Winograd and Thordarson (1975) as the valley-fill, tuff, and upper and lower carbonate aquifers; however, only the shallow groundwater found in the valley fill is of interest to this study. Quittmeyer, (2000) also noted occurrences of perched water in the Amargosa region within the valley fill.

Purpose and Objectives

The purpose of this study is to evaluate the effectiveness and feasibility of frequency electromagnetic (FEM) conductivity soundings and shallow seismic reflection to measure depth to shallow water and its vertical and lateral variability in arid environments with elevated soil salinity. The objectives are first to determine how FEM conductivity data can be modeled to create a depth profile that sufficiently correlates with the actual conductivity profile; second, to determine how conductivity profiles can be interpreted to correspond with shallow water surfaces in arid regions with elevated salinity; third, to determine how shallow high-resolution seismic reflection can be used in combination with EM models to improve interpretations of EM conductivity models of the shallow water table, and; fourth, to evaluate these methods' effectiveness and feasibility for use on larger scale hydrogeological investigations such as evapotranspiration estimates.

Previous Studies and Significance of Project

Numerous studies on the hydrogeology of the Amargosa Desert have been completed as early as the 1950's (Anderson, 2002; Kilroy, 1991; Classen, 1985; Grose and Smith, 1989; Kilroy, 1991; Laczniak et al., 1999; Walker and Eakin, 1963; Winograd and Thordarson, 1975; and references therein). Despite the importance of the shallow valley-fill aquifer, which serves as the main water supply for the Amargosa Desert, there are inconsistencies in reports of depth to water within it. Measurements at Carson Slough, directly adjacent to AMNWR, range from 1 to 10 m (Anderson, 2002; Kilroy, 1991; Laczniak et al., 1999; Walker and Eakin, 1963; Winograd and Thordarson, 1975).

Geophysical methods have been used for many years to solve hydrogeological problems (Kelly, et al. 1993; Reynolds, 1997); however, very little has been done to examine the ability of loop-loop frequency domain EM and seismic to measure depth to groundwater in shallow saline conditions.

EM instrumentation has been used in numerous hydrogeological studies, but typical applications differ from those of this study. There are a variety of EM instruments which are generally selected on the basis of the desired depth of exploration. Small loop loop FEM instruments are generally the tools of choice for shallow (<10 m) EM exploration (Mitsuhata, et al., 2006). FEM instruments are typically used in an effort to determine lateral extent of groundwater (Potts, 1990), mapping groundwater contamination plumes (Al-Tarazi, et al., 2008; Buselli, et al., 1992), mapping subsurface discontinuities (Potts, 1990; Stroh et al., 2001; Sengpiel, 1998), measuring near-surface soil moisture (Sheets and Hendrickx, 1995; Persson and Haridy, 2003), and determining depth to claypan (Brus et al., 1992; Cockx and De Vos, 2007; Doolittle, et al., 1994). In cases where vertical resolution is needed, such as determining hydrostratigraphy or detection of salt water interfaces in freshwater aquifers, transient electromagnetic (TEM) is considered favorable; however, most of these instruments are limited to deeper targets (Fitterman, and Stewart, 1986). Traditionally, TEM instruments are used to explore depths >50 m, and interpretation methods are more complex but have been used with success (Fitterman and Stewart, 1986; Fitterman et al., 1999), although some new nano TEM instruments are capable of investigations in the upper 1-30 m. The shallow limit of TEM accuracy is a function of conductivity, and results in variable resolution in the shallow zone (Urquhart, 2009). The upper 4 m mainly reflects pore fluid salinity (Tan et al., 2007). More detailed explanation of EM theory and principles of operation are given by Nabighian, and Corbett (1991).

Integration of seismic and electromagnetic data has been previously applied in the Amargosa Desert (Louie et al., 1997). Their goal was not for hydrogeological characterization but a similar combination of methods (FEM, TEM, and seismic) were successfully integrated in the characterization of the Pahrump Valley fault zone.

Although seismic reflection and refraction have been used many times to measure depth to water (especially refraction), the seismic method is not typically aimed at imaging ultrashallow (<3 m) layers. There is no guarantee that a capillary fringe will not prevent a reflection from being detected (Kelly and Mares, 1993). However, Baker et al. (2000) performed one such experiment where ultra-shallow seismic reflection was successfully used to measure seasonal fluctuations in sub-meter depth to groundwater near the Arkansas River in Kansas. Their accuracy was within 12 cm; however, their geophone spacing was only 2 inches (5 cm), and their acoustic source was a .22 caliber rifle.

METHODS

Transect Locations

Four 200-m straight-line transects were chosen at the Carson Slough site (Figures 1-B, and 7) so as to correspond to existing piezometers, which served as control points. FEM and seismic data were collected along each line for comparison. One 100-m straight-line transect at the Palmyra site (Figure 1-A) was chosen based on the flatness of the ground surface, the shallow depth to groundwater, and absence of dense vegetation that otherwise covered the area. In order to provide a control transect in an area similar to the Carson Slough site, but with a much simpler structure, FEM and seismic data were collected along a profile at the Palmyra site using the same parameters. Two piezometers were installed near each end of the profile as control points so the geophysical data could be compared with actual depth to water measurements.

Soil Analyses

In order to create cross sections of the vadose zone to upper phreatic zone, soil samples were collected adjacent to piezometer holes at wells 1, 2, and 3 at the Palmyra site and along wells 2, 4, 5, and 6 at the Carson Slough site. Samples were taken approximately every 1-2 ft (0.3-0.6 m) for construction of a cross section of the soil profile, and for further analysis including direct conductivity measurements, x-ray diffraction (XRD) analysis, and analysis of leachate on the flame atomic absorption spectrometer (AA). These data were collected for comparison with geophysical data. The depths associated with the augered soil samples are approximate, due to the shape of the auger bucket which collects soil within a 0.3 m long cylinder with a 0.1 m diameter. Samples were assigned depths corresponding to the middle of the bucket during sampling. The direct conductivity measurements were taken for comparison to EM conductivity profiles in order to confirm the instrument readings. This was done using by making a slurry with 30 g of soil sample and 30 mL of de-ionized water and analyzing it with a YSI brand salinity-conductivity-temperature gauge. XRD analysis for determining quantitative mineralogy was done using procedures outlined by Ebel (2003) for powdered samples using a Scintac Inc XRD and processing the data using the United States Geological Survey (USGS) program “RockJock” (Eberl, 2003). A Perkin Elmer 1500PC atomic absorption spectrometer was used to examine concentrations of Na^+ ions at various depths along the profile of one well. This was done by mixing 40 g of soil sample with 80mL de-ionized water and allowing it to equilibrate, then using the leachates from each sample for analysis (Table 1).

EM Conductivity Soundings

Typically EM hydrogeological studies use a single instrument for data acquisition. For this study three FEM conductivity meters were chosen to achieve the necessary range of penetrations to create a depth profile at each sounding. The three FEM instruments used were the Geonics EM-38 (14.6 kHz with 1-m coil separation), EM-31-SH (9.8 kHz with 2-m coil separation), and EM-34 (6.4 kHz and 1.6 kHz with 10-m and 20-m coil separations respectively. They have effective penetrations of 1.5-m, 3-m, 15-m, and 30-m respectively. This array of instruments allows for 12 conductivity soundings at each point. Measurements with the EM-38 and EM31-SH were taken in both horizontal and vertical dipole orientations at the user's hip height and at the ground surface. The EM-34 was used in vertical and horizontal orientation at 10-m and 20-m coil separations at the ground surface. One 100-m profile of EM data was collected at the Palmyra site with a corresponding seismic profile in October 2008. The EM data at Carson Slough were collected from August 20-30, 2007 over four 200 m profiles with 10-m spacing between soundings. Each profile corresponded with one of the four seismic profiles and at least one monitoring well (Figure 7). The EM profiles extended beyond the seismic profiles on both ends.

The FEM data were processed using Interpex Limited IX1Dv3 software. The Occam inversion smooth model was used to generate 1D conductivity vs. depth profiles for each sounding and 2D conductivity profiles for the entire line (Constable, 1987). The data were modeled with 14 to 20 layers, depending on which number produced the best fit model. The layers increase in thickness with depth because they are modeled on a logarithmic depth scale, resulting in a loss of resolution with depth. Various combinations of data were modeled to determine if more accurate models could be generated by using only horizontal or vertical dipole data, or only specific instruments and it was determined that using all of the data produced the best models.

Seismic Reflection and Refraction

Seismic data were acquired over an eleven day period in August 2007 at Carson Slough and over a three day period in October 2008 at the Palmyra, UT site. The data were acquired along four profiles each between 200 ft (61.0 m) and 325 ft (99.1 m) in length and each corresponding with a section of the four EM lines. Two seismic profiles from Carson Slough are discussed herein, one representing a typically shallow water level (~ 1 m) and one representing a typically deep level (~ 3 m) (profiles 1 and 2, respectively).

Seismic acquisition parameters were chosen for high resolution in the shallow subsurface. These included using a 1-kg mallet source (4.5 kg sledge hammer source when windy conditions created excessive noise), 96 channel, common depth-point (CDP) recording, 28-Hz vertical geophones, 0.125 ms sample rate, field filters: 35-Hz (Palmyra) & 200-Hz (Carson Slough) low-cut, 1 ft (~0.3-m) geophone spacing, and stacking shot records three times to reduce noise.

The data were first converted from SEG-2 to SEG-Y format and assigned 3D geometry. Records were examined for quality and bad traces were deleted. Appropriate mute functions were applied to eliminate first arrivals (direct and head waves) to bring out deeper reflections. The air blast was also muted in order to allow better resolution of very shallow reflections. An Ormsby bandpass filter (100-200-700-900 Hz (zero phase) for Carson Slough; 100-120-300-700 Hz (minimum phase for Palmyra)) was then applied followed by a deconvolution to compress the wavelets and reduce multiple reflections. Post-stack was also applied. Automatic gain control (200-ms window for Carson Slough; 100-ms for Palmyra) was applied, followed by CDP stacking, velocity analysis and conversion from time to depth. The stacks are displayed with a 5-trace weighted mix in order to suppress low-apparent velocity noise. Since our targets were very shallow (< 5 m), depth conversion was applied using a velocity appropriate for the uppermost soils, based on the direct arrival or the lowest normal move-out (NMO) velocity. Note that no elevation static correction is applied so as to afford direct comparison with the EM modeling, which is referenced to the ground surface. Elevation changes along the profiles were relatively small (usually < 0.5 m). Each CDP section was stacked with an NMO velocity appropriate to the water level depth expected from the nearest well(s). In addition to processing the seismic data for CDP reflection, classical modeling of the direct arrivals and head waves was also performed for a two-layer case and the results plotted directly on the CDP stacked sections.

RESULTS

Palmyra Site

Soil and Water

The soil profiles from all three augered holes have an identical progression of soil types (Figure 2). The upper 2.1 m is silt with a silty sand layer from approximately 2.1 to 2.4 m followed by silt increasing in moisture content until saturation. Water levels were 9.5 ft (2.9 m) in well 1 and 9.8 ft (3 m) in well 2 (Table 3). Samples from wells 1 and 2 were used to make a slurry from which direct measurements of conductivity were taken for comparison to EM conductivity profiles (Figure 3). Samples from Palmyra well 1 and Carson Slough well 4 were also analyzed by XRD to determine mineralogy and attempt to quantify salts; however, salinity concentrations were too low to quantify accurately. The approximate mineralogy, determined by XRD analysis, can be found in Appendix A-1 and A-2. Major minerals include quartz, Na-smectite, calcite, dolomite, and anorthoclase feldspar. Results from AA analysis of leachate from Palmyra well 1 samples show Na^+ concentrations generally increasing with depth and decreasing at or just above the water table (Figure 4). These soil analyses were useful in comparison and confirmation of geophysical data as well as confirming the link between salinity and conductivity trends.

EM Model Results

Modeling of FEM data was performed along the line indicated in Figure 1-A. Results show that the conductivity vs. depth profile of the first nine stations along the line were similar both in conductivity magnitudes and pattern over depth in the upper 6 m while results for station 10 (located on a compacted dirt road) were less similar outside of the 2-6 m range. The overall trend in conductivity shows a gradual increase with increasing depth up to approximately 3 m. At 3 m conductivity drops and remains relatively consistent to the bottom of the profile at 30 m (Figure 5), although, less confidence is put in these data past a depth of 6 m due to a decrease in resolution with depth and interference with higher conductivity of the shallower zones. Raw data can be examined in Appendix A-3. Overall, the EM data quality for the Palmyra site was high quality and provided a good calibration for EM analysis and modeling at Carson Slough. Modeled EM values range from 10-20 mS/m at the surface, to 100-150 mS/m in the mid-vadose zone, to ~1000 mS/m at the peak above the vadose-phreatic boundary.

Seismic Results

One seismic survey was performed at the Palmyra site (Figure 6) located along the same line as the EM profile (Figure 1-B) and extended for approximately 70 m from stations 2 to 9. Measured depth to water at Palmyra well 1 (EM station 2), on the northeast end of the seismic line, was 2.9 m and water depth at Palmyra well 2, on the southwest end of the line, was 3.0 m. The slight convex curvature of the reflection is due to a slight concave slope in the ground surface. Data quality was good and showed coherent reflections. In comparison with line 2 at Carson Slough, where water a surface was found at a similar depth, the reflections appear to be more coherent and continuous (Figures 13). Measured depth to water in wells and interpreted depth to water table from the EM data is plotted in Figure 6-B. EM interpretations correlate very well with measured water depth and a strong reflector.

Carson Slough Site

Soil and Water

Locations of wells 1 through 9 and lines 1 through 4 can be found on Figure 7. Unified soil classification system (USCS) symbols for various depths of Carson Slough wells 1 through 9 can be found on Table 2. It is clear from these classifications that the subsurface is fairly heterogeneous (Figure 8), relative to the Palmyra site. Some layers are discontinuous, segmented, and some are only present in a single well. Most of the wells contain swelling clays toward the bottom. Some additional holes were augered and were rejected at hardened caliche layers. The variation in water depths in the closely spaced wells was too great to be considered as representing a simple unconfined system. Several additional investigative holes were augered to determine if the system was confined and some areas had up to 4 ft (1.2 m) of pressure head and some have none, showing that there are areas that are confined. These holes were not augered during the time of geophysical data collection and water levels are transient in this area so this pressure head could be different than pressure head at the time of geophysical data acquisition. Table 3 shows the well data for depth to potentiometric surface and depth to saturated layers where data are available.

Soil samples from wells 4 and 5 were used to make direct conductivity measurements using a soil-water slurry. These measurements show that conductivity is higher in the lower vadose zone than in the upper phreatic zone, and can be compared to EM modeled results (Figure 9). Soil samples from well 4 were analyzed by XRD for quantification of minerals. Major minerals include calcite, dolomite, illite, quartz, and anorthoclase feldspar.

EM Model Results

FEM results for Carson Slough were less consistent than those at Palmyra, as expected due to the geological simplicity of the latter. Lines 1 and 2 are displayed (Figure 10 and 11) to demonstrate conductivity profiles with shallow water at two different depths. There is a high degree of variability in both magnitude and conductivity patterns over depth; however, they do show that there is generally a conductivity high above the phreatic zone. The spacing between the high and low conductivities is difficult to correlate to water surfaces because the depth to water appears to be related to different parts of the conductivity trend depending on the location. Modeled EM results for wells 4 and 5 are shown in Figure 11. Values from these models were plotted next to measured values from soil samples for comparison on Figure 9. Additional EM profiles for the other lines can be found in Appendix A-4. Modeled values for conductivity range from 10-30 mS/m at the surface, to 250-500 mS/m in the mid-vadose zone, to 500-1000 mS/m at the peak above the vadose-phreatic boundary.

Seismic Results

Four seismic lines were included in this survey, but only profiles 1 and 2 are discussed as mentioned above (Figures 12 and 13). The data ranges in quality from moderate to good, due mainly to varying noise levels from wind, which usually increased throughout any day. Field filters, stacking of multiple shot records, and data processing were used to help reduce the influence of wind noise. Each of the four profiles shows shallow reflections in the depth range expected for water levels observed in the wells.

Seismic reflections can usually be correlated with water level measurements from the piezometers. However, these measurements may represent the pieziometric surface, and not the actual depth to saturation, and thus the geophysical detection of groundwater (e.g., in a confined aquifer) may indicate somewhat greater depths.

Profile 1, the northernmost of the four profiles (Figure 12), was surveyed over an active drainage (but dry at the time of the survey) where water level depth in the well was minimal. Shallow reflections with good continuity from the low-velocity field portion of the wave field can be traced across the profile (Figure 12). The refraction model for this line (Figure 12-B) appears to correlate reasonably well with a shallow reflection and measured water level in well 3. Interpretations of depth to water surface from EM models are plotted on the seismic profile for comparison (Figure 12-B). The EM interpretations show a higher degree of variably than the seismic data with a discrepancy of up to 2 m.

Seismic Profile 2 is located just east of an intermittent stream (Figure 1-B) and traverses an area where the water is considerably deeper than profile 1. The low-velocity field, above the refraction model (Figure 13-B), produced poorly expressed reflectivity; however, the high-velocity field, below the refraction model-based depth to a rigid surface (Figure 13) produced an onset of stronger reflectivity arriving between 3 and 4 m below ground surface. Reflections for profile 2 were less coherent and less continuous than those of profile 1. The piezometric surface at well 4 was at 2.8 m below ground and there appeared to be no pressure head. This depth approximately matches the onset of reflectivity in the center of the profile. Depth to piezometric head at well 5, located on the west end of the profile, was 1.96 m and an additional investigative hole was augered later and found that well 5 is in a confined system where depth to saturation is 2.26 m, shallower than the onset of reflectivity. The refraction model (Figure 13-B) shows that the depth to the first rigid boundary changes from 4 m on the east end of the profile to < 1 m on the west end. The upper layer on the east half of the profile could represent a fluvial channel, which is consistent with its location in an ephemeral braided stream system. The dashed line represents a possible second rigid layer at a depth of 3.8 m. Coherency of reflections above the refraction model is lower than below it. EM interpretations to water surface are also plotted on Figure 13-B and show more variability in depth than reflections, but less variability than the refraction model; however, it corresponds fairly well with the second refraction boundary on the west half of the profile.

DISCUSSION

The shallow water surfaces and elevated soil salinity create a challenging environment for geophysical exploration of the groundwater system. Unconsolidated lacustrine and alluvial sediments can result in rapid attenuation of acoustic energy and a well-developed capillary fringe just above the phreatic zone can result in diminished velocity contrast by causing a gradational change in velocity rather than a clear boundary. High soil salinity results in high conductivity, which decreases the accuracy of EM measurements as depth increases (Callegary, et al., 2007). Despite these problems the data show that EM and shallow seismic methods are promising in measuring the configuration of the groundwater system when constrained by strategically acquired ground truth.

The fact that the EM results varied considerably between the two sites in this investigation suggests that the interpretation of EM data must be site specific. There is not a universal conductivity that defines when a porous medium is saturated, nor is there a universal trend of conductivity vs. depth. Local soil conditions must be taken into account to determine depth to water when examining contrasts in conductivity vs. depth. If there is a significant contrast in conductivity between the vadose and phreatic zones then these contrasts can be interpreted to correlate to a water surface and their depth can be inferred from the Occam inversion 1D profiles.

In arid areas with high concentrations of soluble salts in the soil, the conductivity of the soil is dominated by salinity. Williams and Baker (1982) concluded that when measuring apparent conductivity, salinity can account for 65-70% of the electromagnetic response. Changes in subsurface conductivity are typically related to changes in the dominant factor (Cook et al., 1992), which, in this case, is salinity. In both sites for this study there appeared to be a conductivity high in the vadose zone and a drop in conductivity in the phreatic zone, although the degree of change varies. At Carson Slough well 4 (Figure 9-A) the modeled change in conductivity exceeds 800 mS/m and at Carson Slough well 5 (Figure 9-B) the modeled change in conductivity is only 100 mS/m. This change in conductivity can be related to vertical changes in salinity within the soil profile. Gilman and Bear (1994) confirmed that salinization of the vadose zone is common in arid regions, particularly where water table is shallow, due to evaporation of soil moisture. Dissolved salts present in small quantities in groundwater precipitate out into the soil as the water is drawn up by capillary rise and evaporated (Forkutsa et al., 2009; Gilman and Bear, 1994).

Salts were not concentrated enough in borehole samples to be measured with accuracy using x-ray diffraction; however, quantification of salts, relative to other samples from the same column, was achieved by a leaching experiment. The leachate from vadose zone samples show a generalized increase in Na^+ ion concentrations as depth increases and an abrupt drop in Na^+ ion concentration at the phreatic zone (Figure 4). This confirms the link between salinity in the soil and conductivity measured either directly, or by electromagnetic response.

Small vertical fluctuations in Na^+ ion concentration and fluctuations in directly measured conductivity (Figures 3 and 9) were visible; however, the general trend for each set of measurements is similar. The EM models do not show these small vertical fluctuations because the nature of the soundings measures apparent conductivity over a given volume and the Occam's inversion produces a smooth model which cannot resolve minor fluctuations in a general trend. Overall vertical trends can be picked up and modeled accurately in the case that the subsurface is fairly horizontally homogeneous, such as at the Palmyra site.

At the Palmyra site, EM conductivity vs. depth profiles at each station were modeled and analyzed. Each measurement in this line had a very similar electromagnetic response at its respective depth. This is likely due to the laterally homogeneous soil profile and salinity distribution. Because the aquifer is relatively homogeneous and unconfined, it is expected that salinization due to capillary rise and evaporation would be consistent across the entire area resulting in laterally comparable salinity concentrations. For this line the water table corresponded to the point on the profile where conductivity drops from its peak. Using this pattern, the depth to water was modeled across the line at a depth of 3 m, which is well within a reasonable range of the piezometer water levels of 2.9 m at well 1 and 3.0 m at well 2.

EM interpretation at Carson Slough was more complex. Before EM models could be understood, an interpretation of the subsurface needed to be made to know how conductivity could vary over the profiles. Several factors contribute to the interpretation that the aquifer is not a continuous system, but is made up of saturated channels flowing perpendicular to the profiles. The variation in potentiometric surface over short lateral distances, in combination with the fact that pressure head varies from 0 m to 1.2 m (Table 3) indicates that water systems are not connected. Water temperature and conductivity are also inconsistent across single profiles

(Table 3). Water levels in several wells were measured 2 months after the collection of geophysical data indicating that depth to water increased by varying amounts in wells 4 and 5, but decreased by varying amounts in wells 1, 2, and 6 (Table 3). The current geologic setting of the profiles is in an ephemeral river system that only flows at the surface after a storm (Tanko and Glancy, 2001). It seems logical that the subsurface would contain buried channel systems at various depths, some of which may or may not be confined by fine clays (Figure 14). A similar arid environment with buried fluvial channels and fine clays can be found in the Okavango Delta, Botswana (Milzo et al., 2009; Tooth and McCarthy, 2007)

Vertical salinity distribution in the Carson Slough area cannot be expected to be laterally consistent where water surfaces, confining units, and soil types are not laterally consistent. For this reason, conductivity distribution, although similar, is not consistent over the length of any of the four EM profiles at Carson Slough (Figures 10 and 11). Although there is a conductivity high above the saturated zone, in some cases the high is immediately above the water, as seen at wells 1 and 2 at the Palmyra site (Figure 3), and in other cases it is 1-2 m above the water, as seen at Carson Sough wells 4 and 5 (Figure 9). Because not enough piezometer control is present to compare to each pattern of conductivity distribution, it is difficult to interpret an exact depth to water with confidence. If depth to water is interpreted across an entire profile at the point where conductivity drops, one can see that the depths are fairly inconsistent (Figure 15). This is most likely influenced by the natural variations in depth to water across the profile, the thickness of the saturated zones, and the seasonal fluctuations in depth to water. Seasonal changes in water depths could result in perpetual vertical re-distribution of salinity. However, since water levels measured at Carson Slough suggest that the amount of change, and even the direction of change in water level varies across a short distance, the salinity re-distribution will also vary laterally.

The complications of heterogeneity, segmented thin reservoirs, and seasonal water level changes make FEM difficult to use for interpreting depth to water at Carson Slough unless calibrating information such as occasional drill holes and /or seismic data are available. It appears that using an interpretation that saturated depth corresponds with the depth where the modeled conductivity drops from its peak is accurate to within approximately ± 2 m. This uncertainly is difficult to gauge because it is directly proportional to water surface fluctuation and heterogeneity in soil type and salinity concentration, which are poorly constrained in the study area. However, because conductivity is linked to salinity, and soluble salts are more likely to build up in areas where there is less direct communication with surface water, areas of higher conductivity could be interpreted as areas with more confined systems, where areas with lower conductivity could be interpreted as zones with greater surface water-ground water interaction.

The Palmyra site was essential in providing more of a "standard" site for exploring a shallow water table in saline conditions, but with a more homogeneous geological setting. The seismic profile at Palmyra was very successful in producing a simple reflection and head wave. Despite the shallow nature of the target, and the possibility of the capillary fringe preventing contrast in acoustic impedance at the water table, a strong reflection is apparent that corresponds to the water depth as measured in the two piezometers (Figure 6-B). The resolution of the seismic line is finer than that of the EM profiles, and because the CDP surface station spacing is 1 ft (~0.3 M) and EM stations were spaced at 10 m, the seismic line is far more complete for the interval over which it was applied. As discussed above, the slight convex upward nature of the reflection is a result of a slight concave nature of the ground surface over a constant water table.

This indicates that, relative to ground surface, depth to water is slightly less in the middle of the line. This detail could not be resolved using the EM models, which were used to interpret a depth of 3 m to water table across the entire line.

In the Carson Slough seismic profiles, shallow reflections, supported by velocity-depth modeling of head waves and direct arrivals, indicate some correlation with depth to water in piezometers on the lines (Figures 12 and 13). However, some piezometers have water levels that do not correlate with any reflections. The profiles show that there is much more heterogeneity in the Carson Slough area than in the Palmyra site. For example, shallow reflections produced using the low-velocity field from Profile 1 show some undulation and curvature (Figure 12). Reflections in profile 2 are discontinuous and truncated in places (Figure 13), which could be a representation of buried stream channels flowing at a high angle to the profile. The seismic method in Carson Slough is promising, although requires piezometer control and a priori understanding of where confining units may be.

CONCLUSIONS

The testing of FEM and seismic methods to measure depth to groundwater in two different areas allowed for comparison of the effectiveness of the methods in two arid to semi-arid environments with elevated soil salinity that vary significantly in terms of subsurface complexity. This allowed us to test the two end members of probable situations where these methods could be useful while staying within the range of the project's purpose to evaluate their feasibility in arid saline conditions.

FEM soundings (Figures 5 and 11) were found to show similar patterns with measurements taken from actual soil samples (Figures 3 and 9) at corresponding locations. The magnitudes of conductivity from FEM models do not exactly match the conductivities measured from soil samples. This is because measurements of conductivity in soil samples were made using a slurry of equal mass of soil to water. Magnitude of the slurry conductivity is dependent on the soil type, soluble salts, and dilution. The dilution prevents this method from measuring the exact conductivity of the soil itself but, because the dilution was constant, it gives relative magnitudes of the samples. This particular experiment was meant to show that the pattern of conductivity over depth in EM models sufficiently matches direct measurements at various depths, so relative magnitudes of conductivity were sufficient. The conductivity measurements on soil samples indicate that there is an overall trend, but there are some minor fluctuations within the overall conductivity trend (Figure 3), whereas FEM models show only the general conductivity trend (Figure 5). Soil samples at the Carson Slough site were found to show less similarity with their corresponding FEM profiles than those of the Palmyra site due to difficulty in modeling the heterogeneous conditions at Carson Slough using FEM data.

FEM profiles show patterns of conductivity vs. depth that sufficiently correspond to water table at the Palmyra site where the subsurface is fairly homogeneous. This homogeneity allowed for accommodation of the entire horizontal range of the FEM sounding geometry to be deployed without interference from zones of varying conductivity. The conductivity patterns showed enough contrast between the phreatic and vadose zones to distinguish the boundary. This contrast is due to salinization from capillary rise and evaporation: a process common to arid areas with shallow water. At the Carson Slough site, EM profiles were more challenging to interpret. The high degree of heterogeneity, both vertically, and horizontally, in combination with the minimal piezometer control, large seasonal fluctuations in water depth, and segmented thin reservoirs proved too complex to use FEM models to determine depth to water with the same accuracy as at Palmyra.

Shallow high-resolution seismic methods (reflection and refraction) proved to be very useful as a calibration and independent indicator of depth to saturation at both sites (especially Palmyra, Figure 6). Seismic methods proved to have a higher resolution and showed a greater degree of accuracy over the entire length of the profile than FEM results. The integration of the two methods gives much more confidence in measurements of groundwater depth and configuration when piezometer control is not present.

FEM soundings can be readily modeled to determine depth to shallow groundwater where conditions are relatively horizontally homogeneous with sufficient salinization above the saturated zone. This method would be very practical to use for a large-scale investigation. It has the benefits of user-friendly instrumentation, rapid data collection, and is completely non-invasive. However, because patterns in conductivity, not magnitude, are used to determine depth to water it is necessary to have a calibration point where subsurface conditions change. This could be either a piezometer with a well-documented log, or a shallow seismic profile with sufficient resolution. The shallow high resolution profiles could also be used, but it is not recommended for large areas due to the difficulty and time needed to acquire data of sufficient resolution for shallow exploration.

REFERENCES

Al-Tarazi, E., Rajab, J.A., Al-Naqa, A., El-Waheidi, M., 2008, Detecting leachate plumes and groundwater pollution at Ruseifa municipal landfill utilizing VLF-EM method: Journal of Applied Geophysics, v. 65, pp. 121-131.

Anderson, D.E., 2005, Holocene fluvial geomorphology of the Amargosa River through Amargosa Canyon, California: Earth-Science Reviews, v. 73, pp. 291-307.

Anderson, K.W., 2002, Contribution of local recharge to high flux springs in Death Valley National Park, California-Nevada: Master's thesis, Brigham Young University, 122 p.

Barnhurst, D.O., 2003, A chemical, stable, and radioisotopic investigation of an alluvial-fill groundwater system in a semi-arid environment, southern Utah Valley, Utah, Master's thesis, Brigham Young University, 211 p.

Baker, G. S., Steeples, D. W., Schmeissner, C., and Spikes, K. T., 2000, Ultrashallow seismic reflection monitoring of seasonal fluctuations in the water table: Environmental and Engineering Geoscience, vol. 6, pp. 271 - 277.

Bissell, H.J., 1963, Lake Bonneville: geology of southern Utah Valley, Utah: U.S. Geological Survey Professional Paper 257-B, 35 p.

Buselli, G., Davis, G.B., Barber, C., Heigt, M.I., and Howard, S.H.D., 1992, The application of electromagnetic and electrical methods to groundwater problems in urban environments: Exploration Geophysics, v. 23, pp. 543-555.

Bushman, M., 2008, Contribution of recharge along regional flow paths to discharge at Ash Meadows, Nevada, Master's thesis, Brigham Young University, 119 p.

Callegary, J.B.; Ferre, T.P.A.; and Groom, R.W., 2007, Vertical spatial sensitivity and exploration depth of low-induction-number electromagnetic-induction instruments: Vadose Zone Journal, v. 6, pp. 158-167.

Clark, D.W., and Apple, C.L., 1985, Groundwater Resources of northern Utah Valley, Utah: Utah Department of Natural Resources Technical Publication No. 80, 115 p.

Classen, H.C., 1985, Sources and mechanisms of recharge for ground water in the west-central Amargosa Desert, Nevada- a geochemical interpretation: U.S. Geological Survey Professional Paper 712-F.

Cockx, L. and De Vos, B., 2007, Using the EM38DD soil sensor to delineate clay lenses in a sandy forest soil: Soil Science Society of America Journal, v. 71-4 pp. 1314-1321.

Constable, S.C., Parker, R.L., Constable, C.G., 1987, Occam's inversion: a practical algorithm for generating smooth models from electromagnetic sounding data: Geophysics, v. 52-3, p. 289-300.

Cook, P.G., Walker, G.R., Buselli, G., Potts, I., and Dodds, A.R., 1992, The application of electromagnetic technique to groundwater recharge investigations: Journal of Hydrology, v. 107, pp. 251-265.

Doolittle, J.A., Sudduth, K.A., Kitchen, N.R., and Indorante, S.J., 1994, Estimating depths to claypans using electromagnetic induction methods: Journal of Soil and Water Conservation, v. 49-6, pp. 572-575.

Eberl, D.D., 2003, User's guide to RockJock – a program for determining quantitative mineralogy from powder x-ray diffraction data: U.S. Geological Survey Open-File Report 03-78, 41 p.

Fitterman, D. V., Deszcz-Pan, M., Stoddard, C. E., 1999, Results of time-domain electromagnetic soundings in Everglades National Park, Florida: U.S. Geological Survey, Open-File Report 99-426, pp. 155.

Fitterman, D. V., Stewart, M. T., 1986, Transient electromagnetic sounding for groundwater: Geophysics, v. 51-4, pp. 995-1005.

Forkutsa, I., Sommer, R., Shirokova, Y.I., Lamers, J.P.A., Kienzler, K., Tischbein, B., Martius, C., and Vlek, P.L.G., 2009, Modeling irrigated cotton with shallow groundwater in the Aral Sea Basin of Uzbekistan: Irrigation Science, v. 27, pp. 319-330.

Grose, T., L., and Smith, G. I., 1989, Studies of geology and hydrology in the Basin and Range Province, southwestern United States, for isolation of high-level radioactive waste—Characterization of the Death Valley Region, Nevada and California: U.S. Geological Survey Professional Paper 1370-F, pp. 5-19

Harrill, J.R., 1986, Ground-water storage depletion in Pahrump Valley, NevadaCalifornia, 1962-75: U.S. Geological Survey Water-Supply Paper 2279, 53 p.

Hasselquist, N.J., and Allen, M.F., 2009, Increasing demands on limited water resources: consequences for two endangered plants in Amargosa Valley, USA: American J. of Botany, v. 96-3, pp. 620-626.

Johnston, S.C. and T.A. Zink. 2003. Demographics and ecology of the Amargosa niterwort (*Nitrophila mohavensis*) and Ash Meadows gumplant (*Grindelia fraxino-pratensis*) of the Carson Slough Area. Report to the Bureau of Land Management.

Kelly, W. E., and Mares, S. (Eds.) and Karous, M., Kelly, W. E., Landa, I., Mares, S., Mazac, O., Muller, K., Mullerova, J., 1993, Applied Geophysics in Hydrogeological and Engineering Practice: Elsevier, The Netherlands, 289 p.

Kilroy, K. C., 1991, Groundwater Conditions in Amargosa Desert, Nevada-California, 1952-1957: U.S. Geological Survey, (WRIR 89-4101).

Laczniak and others, 1999, Estimates of Groundwater Discharge as Determined from Measurements of Evapotranspiration , Ash Meadows Area, Nye County, Nevada: U.S. Geological Survey (WRIR 99-4079).

Louie, J., Shields, G., Ichinoise, G., Hasting, M., Plank, G., and Bowman, S., 1997, Shallow geophysical constraints on displacement and segmentation of the Pahrump Valley Fault Zone, California-Nevada border: Submitted to Proceedings of the Basin and Range Province Seismic Hazards Summit for publication by the Utah Geological Survey, Cedar City, Utah. url: http://www.seismo.unr.edu/ftp/pub/louie/talks/lvsh/brshs-ed.pdf

Milzow, C., Kgotlhang, L., Kinzelbach, W., Meier, P., and Bauer-Gottwein, P., 2009, The role of remote sensing in hydrological modeling of the Okavango Delta, Botswana: Journal of Environmental Management, v. 90, pp. 2252-2260.

Nabighian, M.N. and Corbett, J.D., (editors) 1991, *Electromagnetic Methods in Applied Geophysics*: Society Of Exploration Geophysicists, Tulsa, Oklahoma, 992 p.

Persson, M. and Haridy, S., 2003, Estimating water content from electrical conductivity measurements with short time-domain reflectometry probes: Soil Science Society of America Journal, v. 67 pp. 478-482.

Potts, I. W., 1990, Use of the EM-34 instrument in groundwater exploration in the Shepparton region: Australian Journal of Soil Research, v. 28, pp. 433-442.

Reynolds, J.M., 1997, An Introduction to Applied and Environmental Geophysics: Wiley, New York, 796 p.

Rhoades, J.D., 1993, Electrical conductivity methods for measuring and mapping soil salinity: Advances in Agronomy, v. 49, pp.201-251.

Sada, D.W., 1990, Recovery plan for the endangered and threatened species of Ash Meadows, Nevada: U. S. Fish and Wildlife Service, Portland.

Sanderson, I.D. 2002, Ground-water sensitivity and vulnerability to pesticides, Utah and Goshen Valleys, Utah County, Utah: Utah Geological Survey Miscellaneous Publication 02-10, 30 p.

Sengpiel, K., 1988, Results of airborne EM groundwater exploration in a desert area using the centroid depth algorithm for evaluation: Natuurwetenschappelijk Tijdschrift, v. 70, pp. 349-356.

Sheets, K.R., and Hendrickx, J.M.H., 1995, Noninvasive soil water content measurement using electromagnetic induction: Water Resources Research, v. 31(10), pp. 2401-2409.

Sparks, D.L., 2003, Environmental Soil Chemistry: Academic Press, San Diego, CA, 352 p.

Stroh, J. C., Archer, S., Doolittle, J. A., and Wilding, L., 2001, Detection of edaphic discontinuities with ground-penetrating radar and electromagnetic induction: Landscape Ecology, vol. 16, pp. 377-390.

Stonestrom, D.A., Prudic, D.E., Walvoord, M.A., Abraham, J.D., Stwart-Deaker, A.E., Glancy, P.A., Constantz, J., Laczniak, R.J., and Andraski, B.J., 2007, Rocused ground-water recharge in the Amargosa Desert Basin: US Geological Survey Professional Paper 1703, p. 107-136

Sweetkind, D.S., Dikerson, R.P., Blakely, and R.J., Denning, P.D., 2001, Interpretive geologic cross sections for the Death Valley regional flow system and surrounding areas, Nevada and California, US Geological Survey Miscellaneous Field Sudies Map MF-2370

Quittmeyer, R.C., 2000, Yucca Mountain site description: Prepared for U.S. Department of Energy, Prepared by TRW Environmental Safety Systems Inc., TDR-CRW-GS-000001 REV 01

Tan, K., Berens, V., Hatch, M., and Lawrie, K., 2007, Determining the suitability of in-stream nanoTEM for delineating zones of salt accession to the River Murray: a review of survey results from Loxton, South Australia: Cooperative Research Centre for Landscape Environments and Mineral Exploration Open File Report, Report: 192, 24 p.

Tanko, D.J., and Glancy, P.A., 2001, Flooding in the Amargosa River drainage basin, February 23-24, 1998, southern Nevada and eastern California including the Nevada test site: US Geological Survey Fact Sheet 036-01.

Tooth, S., and McCarthy, T.S., 2007, Wetlands in drylands: geomorphological and sedimentological characteristics, with emphasis on examples from southern Africa: Progress in Physical Geography, vol. 3, no. 1, pp. 3-41.

Urquhart, S., 2009, personal communication, Zonge Engineering, 3322 E Fort Lowell Rd Tucson AZ, USA 85716

Utah Division of Water Resources, 1997, Utah state water plan, Utah Lake basin: Salt Lake City, Utah Department of Natural Resources, 175 p.

Walker, G.E., and Eakin, T.E., 1963, Geology and Groundwater of the Amargosa Desert, Nevada-California: State of Nevada Department of Conservation and Natural Resources, Division of Water Resources, Water Resources Reconnaissance Series Report 14, 45 p.

Williams, B.G. and G.C. Baker. 1982, An electromagnetic induction technique for reconnaissance surveys of soil salinity hazards: Australian Journal of Soil Research, v. 20, pp. 107-118.

Winograd, I. J., and Thordarson, W., 1975 Hydrogeologic and Hydrochemical Framework, South-Central Great Basin, Nevada-California, with Special Reference to the Nevada Test Site: USGS Professional Paper 712-C.

Workman, J.B., Menges, C.M., Page, W.R., Taylor, E.M., Ekren, E.B., Rowley, P.D., Dixon, G.L., Thompson, R.A., and Write, L.A., 2001, Geologic map of the Death Valley ground-water model area, Nevada and California: U.S. Geological Survey Miscellaneous Field Studies map MF-2381-A, scale 1:250,000.

FIGURES

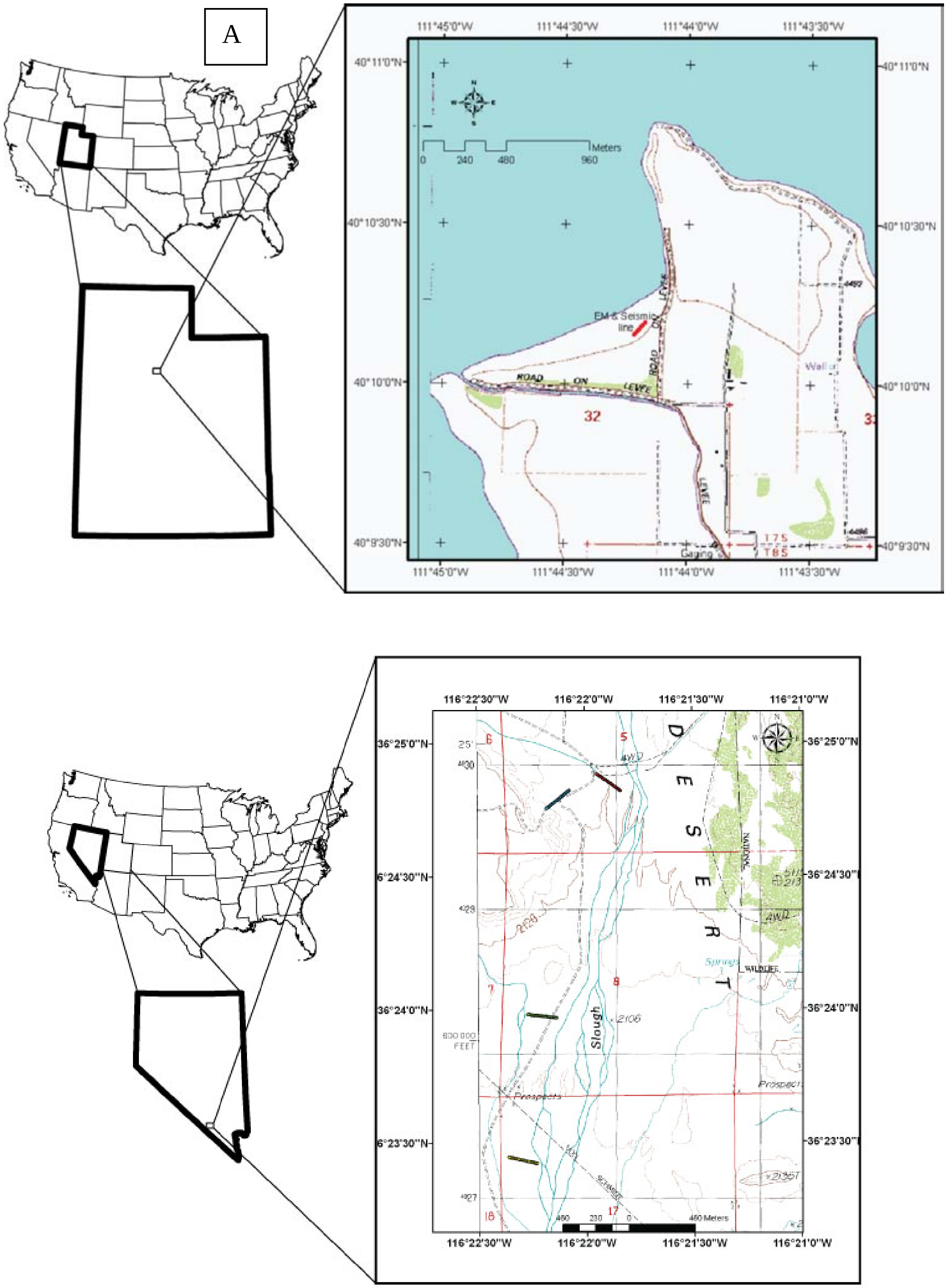

Figure 1. A) Location of EM and seismic reflection profiles for the line at the Palmyra, UT site. B) Location of EM and seismic reflection profiles for lines 1 through 4 at Carson Slough, Nevada site.

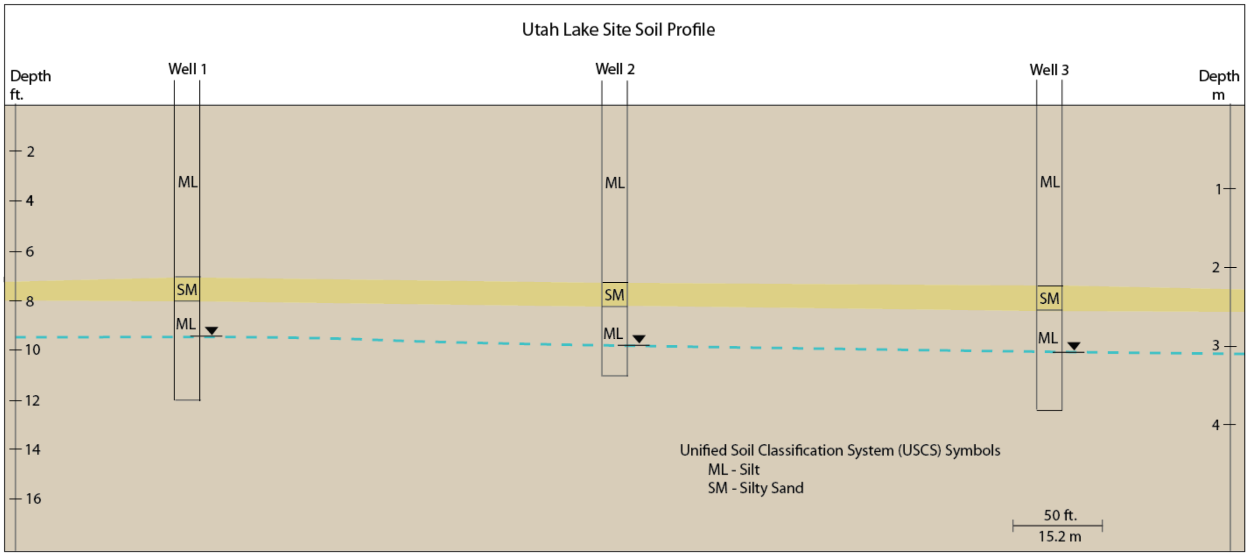

Figure 2. General soil profile for the Palmyra, UT site showing soil types and water table.

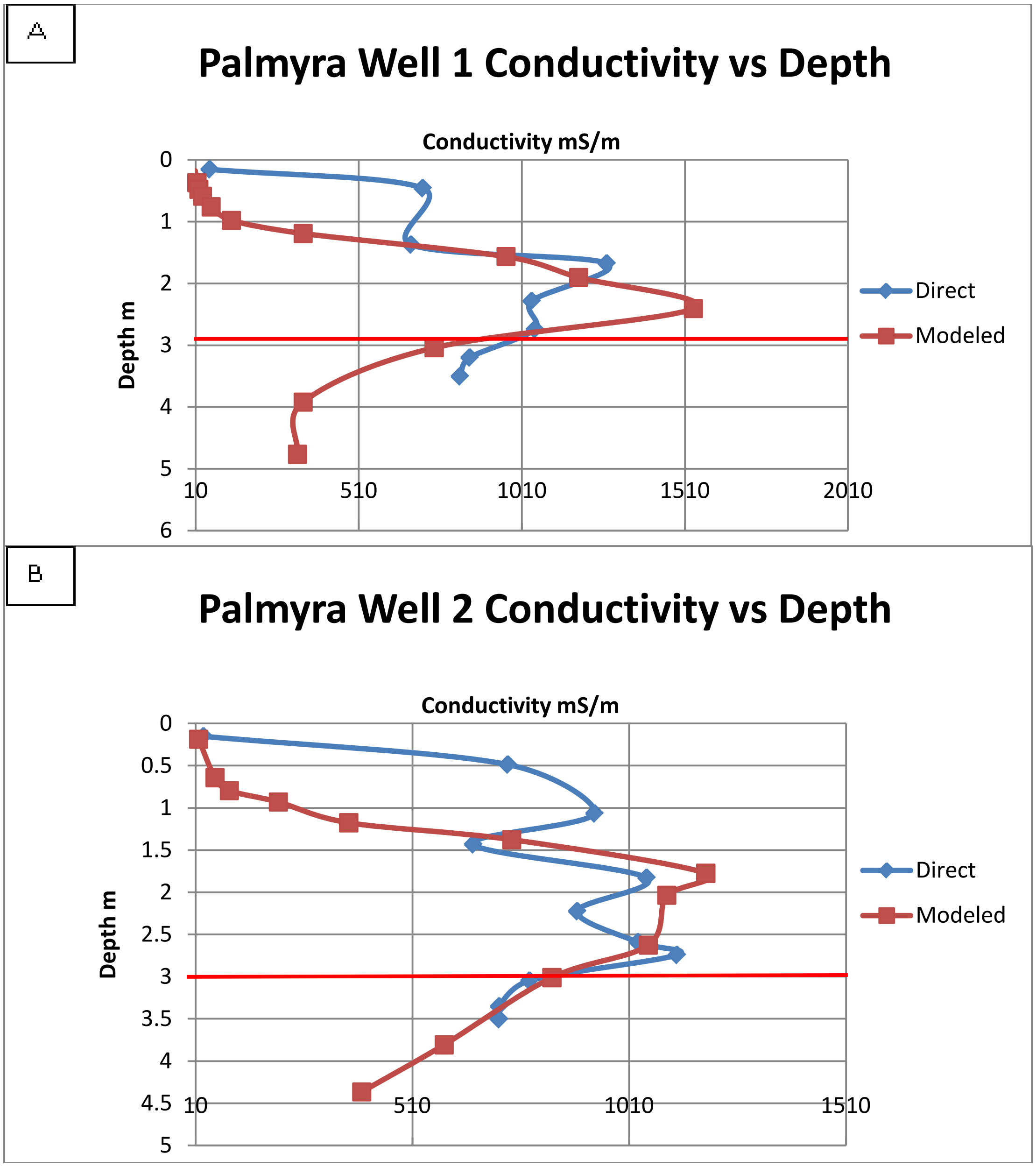

Figure 3. Conductivity measurements from augered holes at Palmyra, UT site. A) Conductivity vs. depth for well 1 where measured depth to water is 9.5 ft. (2.9 m). Blue curve is measured from soil samples in laboratory. Red curve is taken from modeled EM profiles. Red line indicates depth to water table.
B) Conductivity vs depth for well 2 where measured depth to water is 9.8 ft. (3.0 m). Blue curve is measured from soil samples in laboratory. Red curve is taken from modeled EM profiles. All conductivity measurements were made with a YSI conductivity meter from a slurry of 30g of sample with 30 mL of de-ionized water.

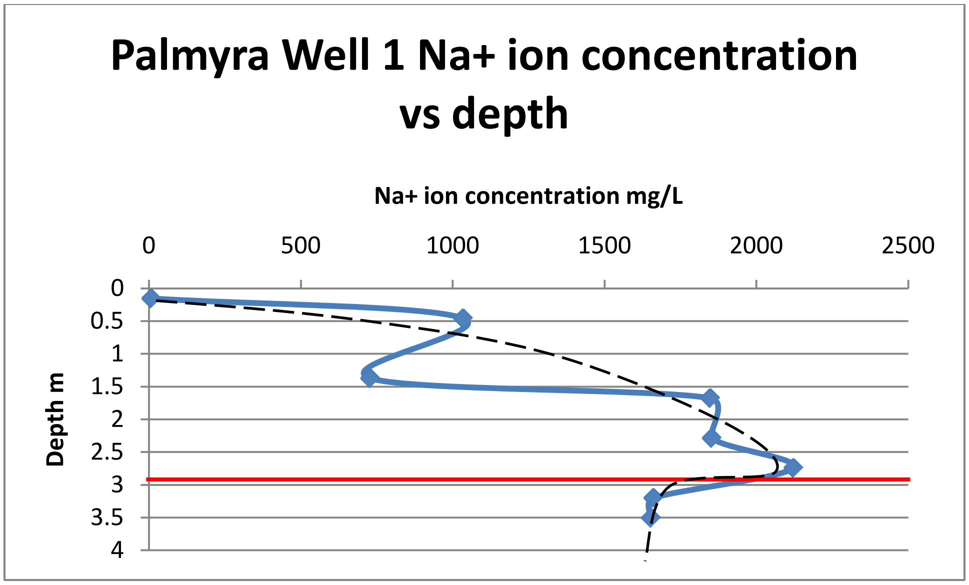

Figure 4. AA analysis of Na^+ concentrations from leachate experiment with soil samples from Palmyra well 1. Red line indicates depth to water table. Dashed line indicates smoothed conductivity trend.

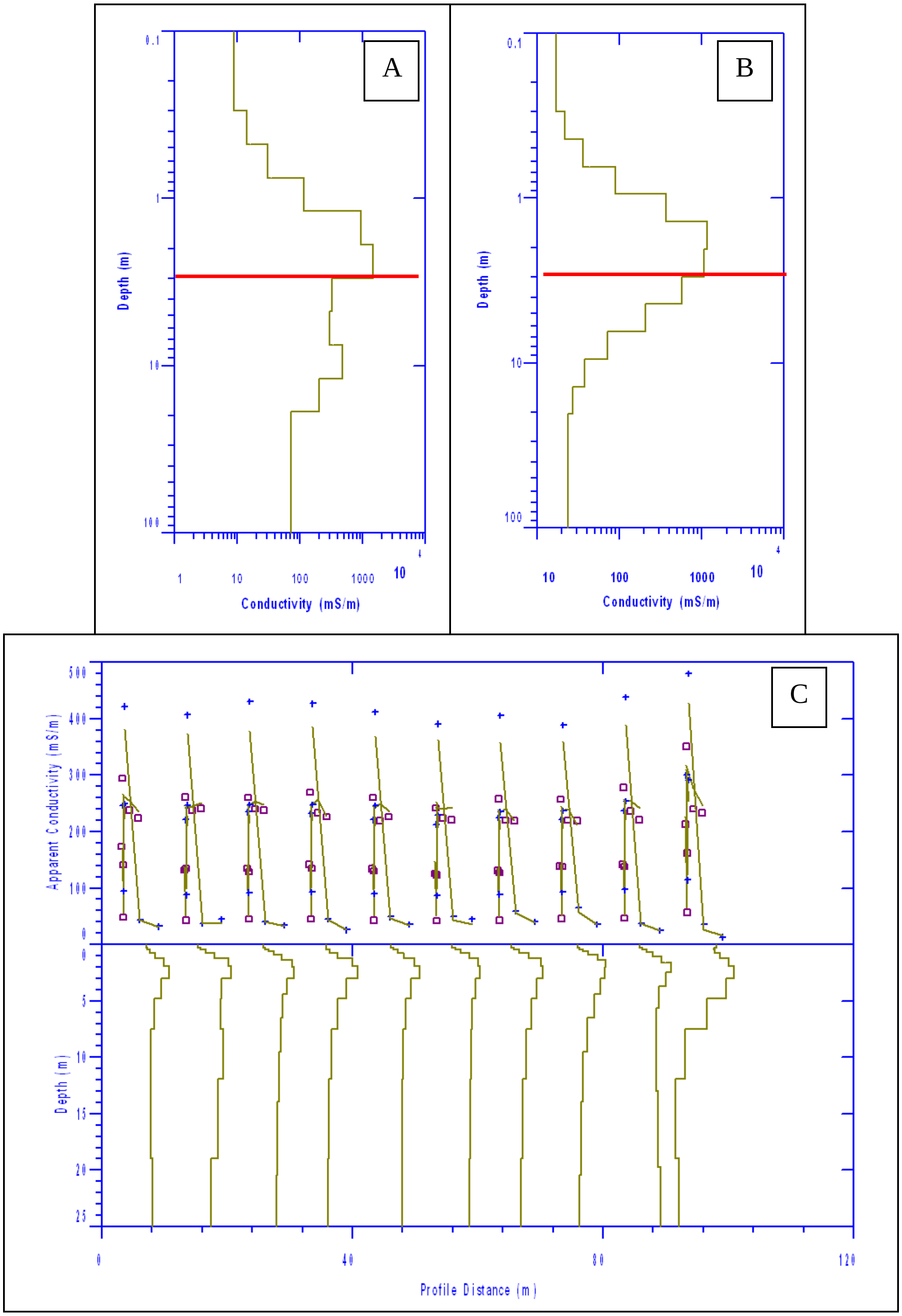

Figure 5. A) EM conductivity vs. depth model for Palmyra well 1 located at station 2 on the profile in Figure 5C. Red line indicates water table. B) EM conductivity vs. depth model for Palmyra well 2 located at station 8 on Figure 5C. Red line indicates water table. C) Profile of EM conductivity data for the entire line with stations 1-10 from left to right. The upper portion indicates conductivity magnitude and distribution of the 12 measurements per station. The lower portion shows the conductivity trend over depth.

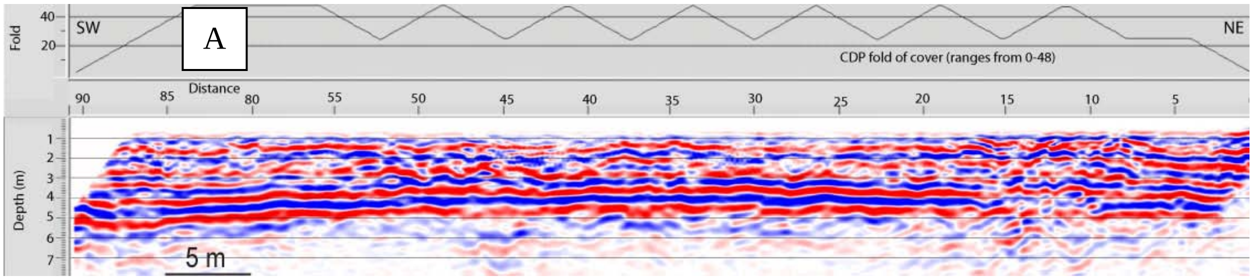

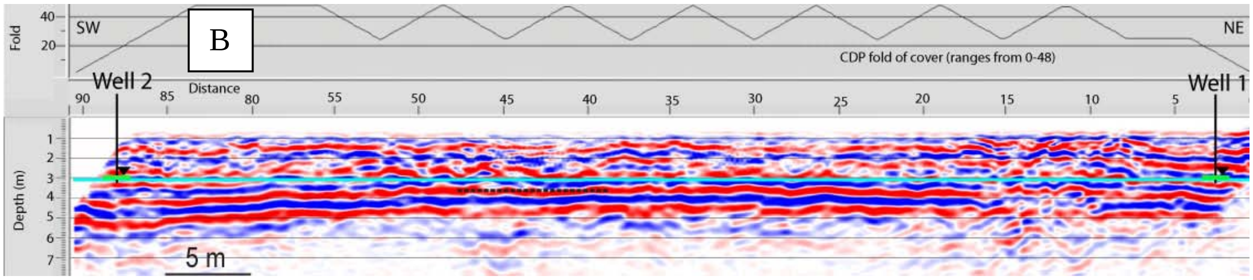

Figure 6. A) Processed seismic line for Palmyra site with fold of cover indicated at the top. Source and receiver spacing is 1 ft (0.3047 m) and CDP spacing is 0.5 ft (0.1524 m).
B) Seismic profile for Palmyra site with location of two wells with their corresponding measured depth to water marked by green line with triangle. EM interpretation of depth to water is marked by the light-blue line. Dashed black line represents depth to first rigid layer determined by refraction models from the shot records.

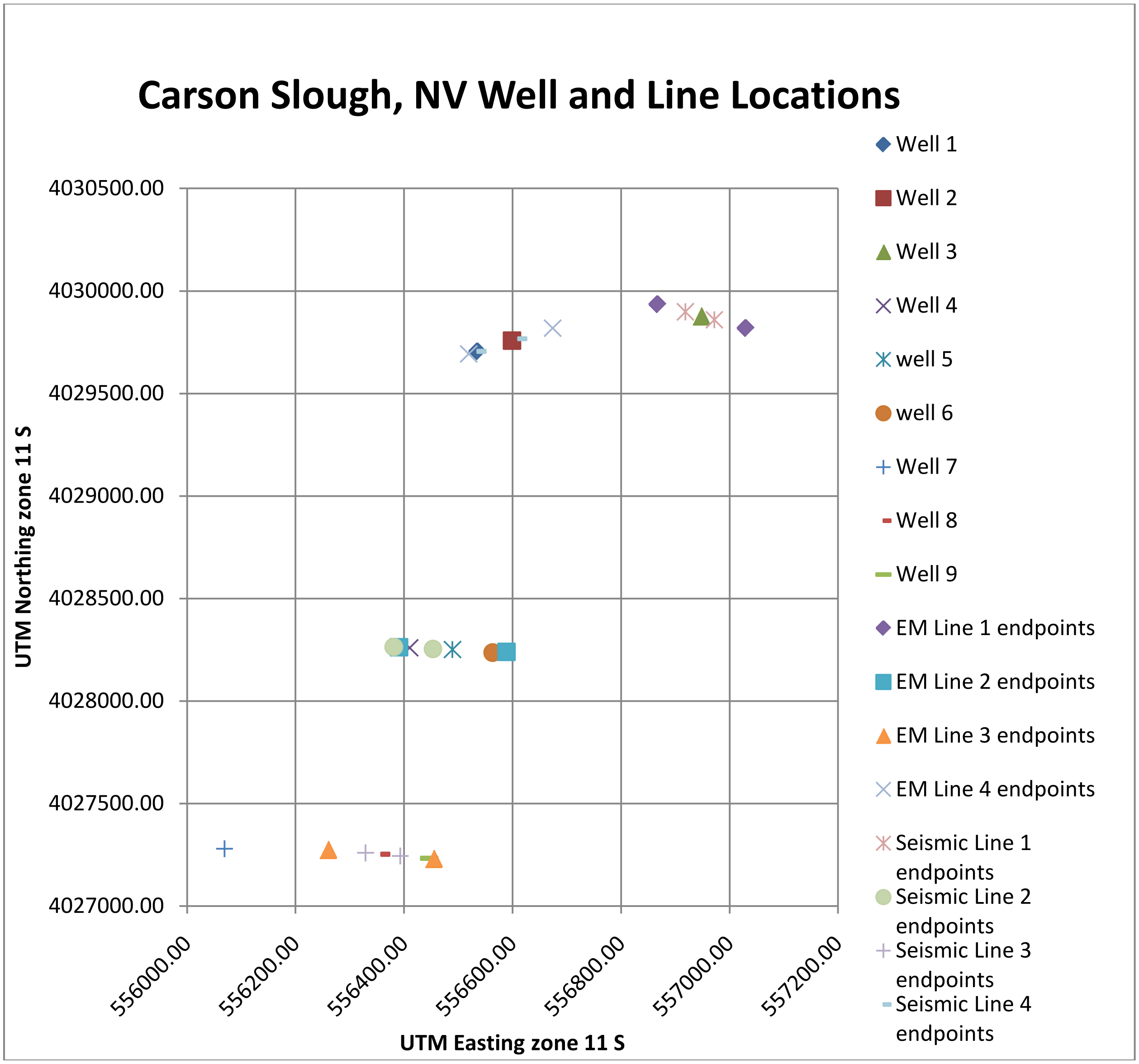

Figure 7. UTM coordinates for wells 1 through 9 and endpoints for lines 1 through 4 at Carson Slough, NV.

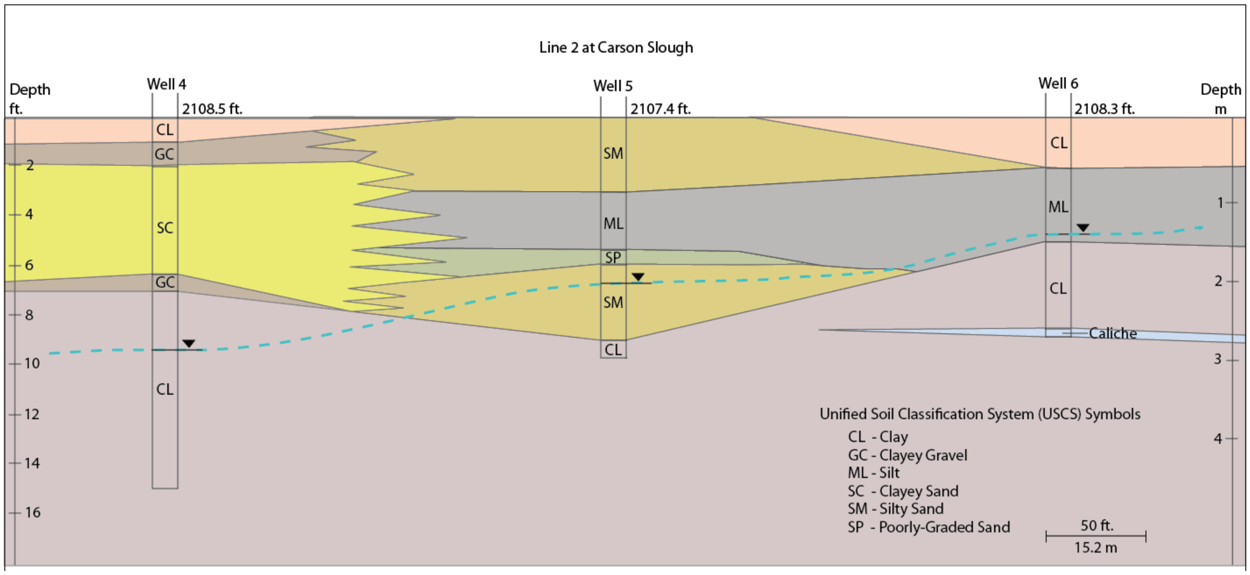

Figure 8. Generalized soil profile for Line 2 at Carson Slough, NV site. Soil column is complex and heterogeneous. Water table is inconsistent

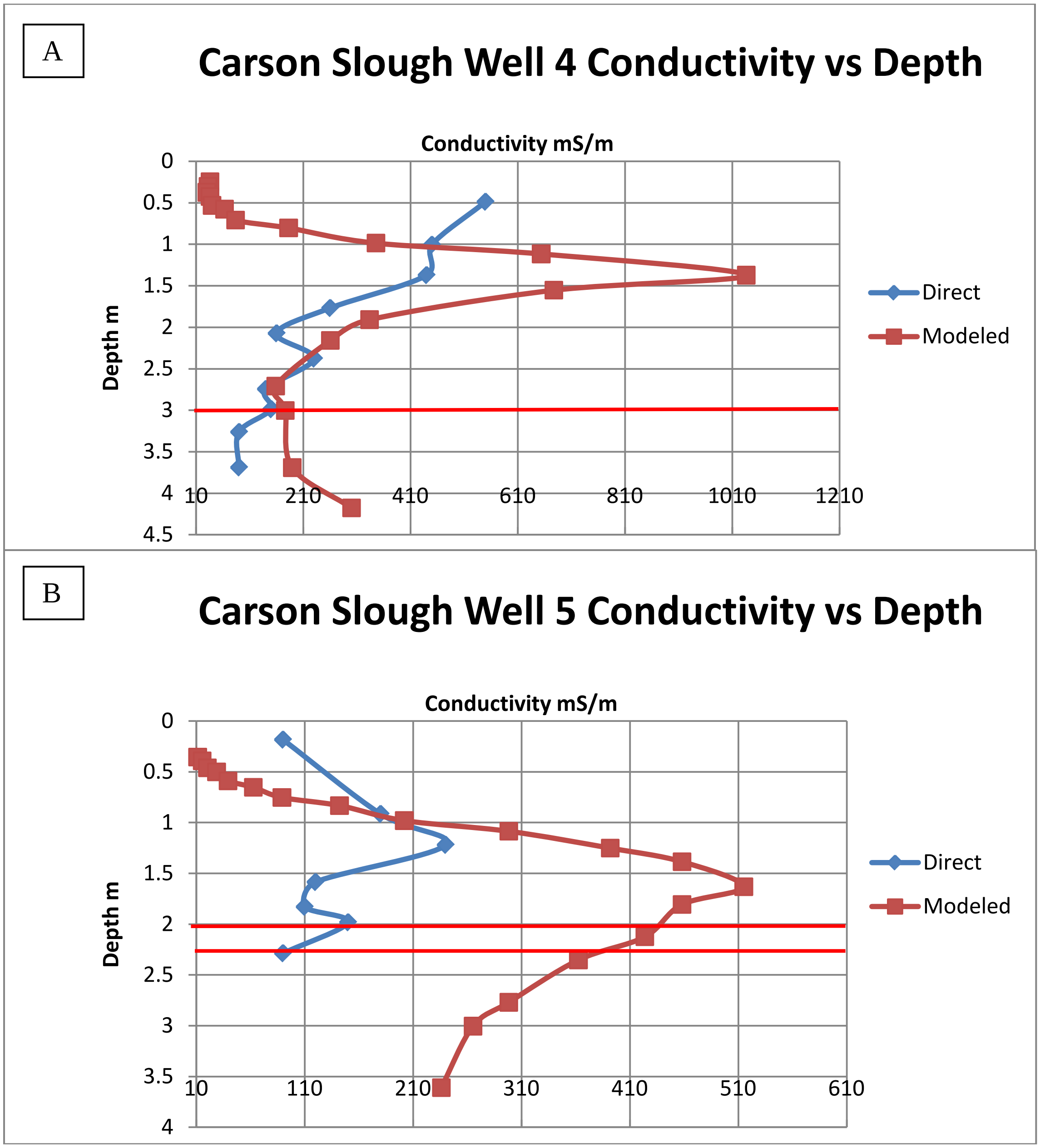

Figure 9. Conductivity measurements from augered adjacent to wells 4 and 5 at Carson Slough, NV. A) Conductivity vs. depth for well 2 where measured depth to pieziometric surface and saturation are both 9.2 ft. (2.8 m) represented by the red line. Blue curve is measured from soil samples in laboratory. Red curve is taken from modeled EM profiles.

B) Conductivity vs. depth for well 5 where measured depth to piezometric surface is 6.4 ft. (2.0 m) and saturation is at 2.25 m represented by the upper and lower red lines respectively. Blue curve is measured from soil samples in laboratory. Red curve is taken from modeled EM profiles. All conductivity measurements were made with a YSI conductivity meter from a slurry of 30g of sample with 30 mL of de-ionized water.

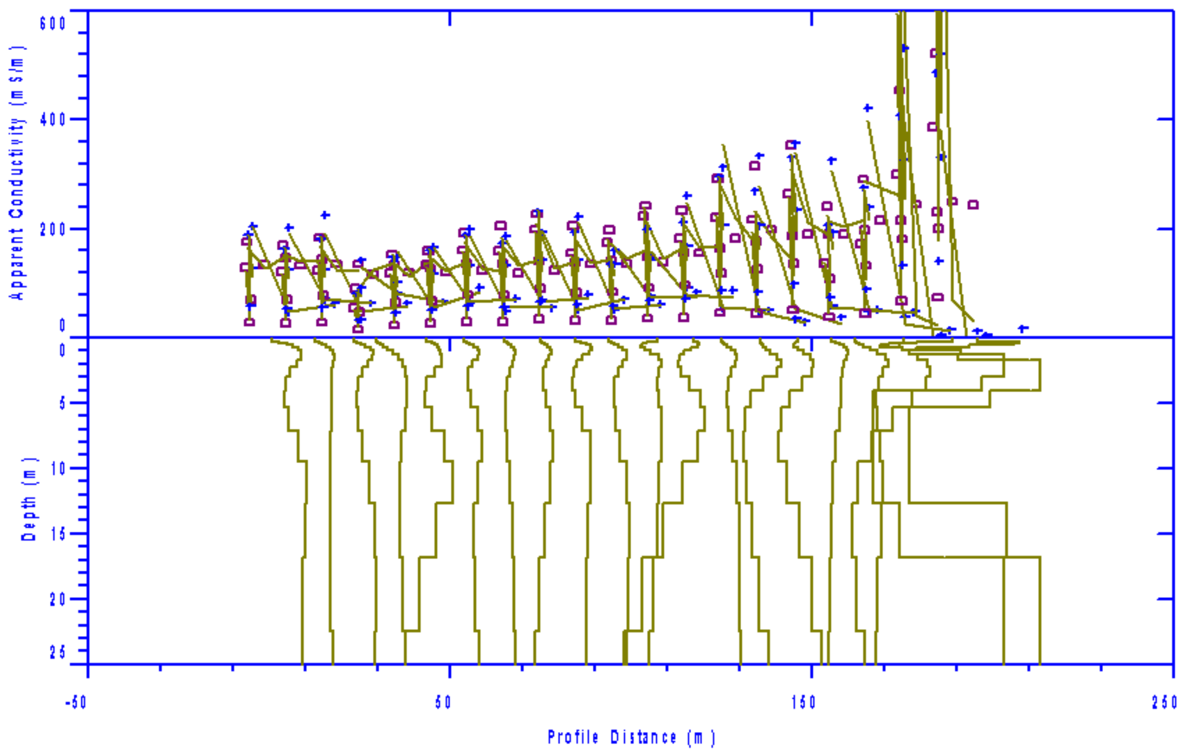

Figure 10. EM conductivity profile for line 1 with stations 1 thorugh 20 from left to right. Station 1 is in the northwest end of the line and station 20 is on the southeast end of the line. The upper portion indicates conductivity magnitude and distribution of the 12 measurements per station. The lower portion shows the conductivity trend over depth.

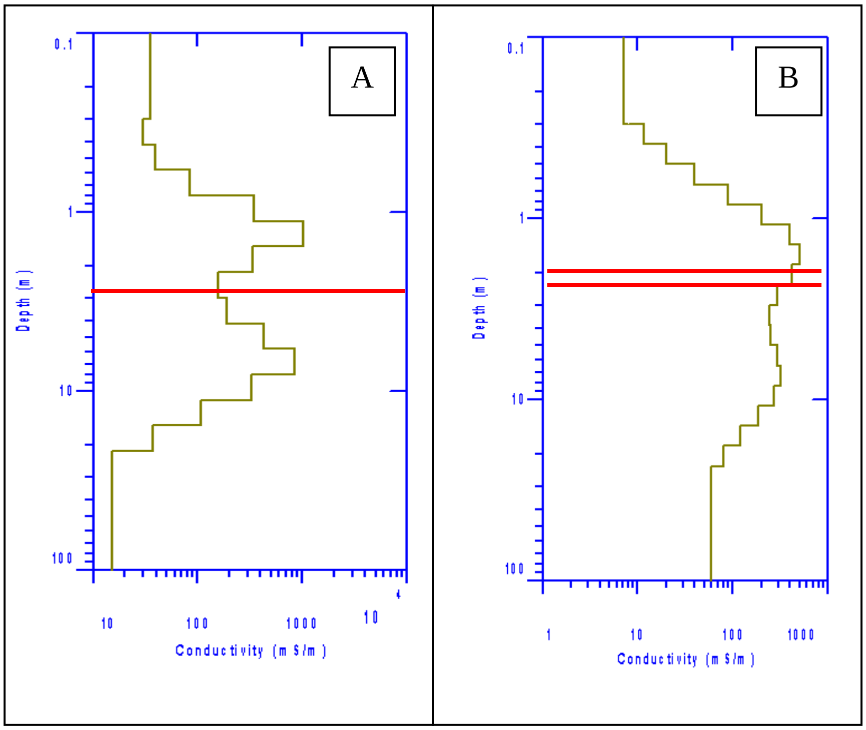

Figure 11. A) EM conductivity vs. depth model for Carson Slough well 4 located at station 3 on Line 2. The red line indicates saturation at 2.9 m. B) EM conductivity vs. depth model for Carson Slough well 5 located at station 11 on Line 2. The upper and lower red lines indicate the potentiometric surface and saturated depth at 2.0 and 2.3 m, respectively.

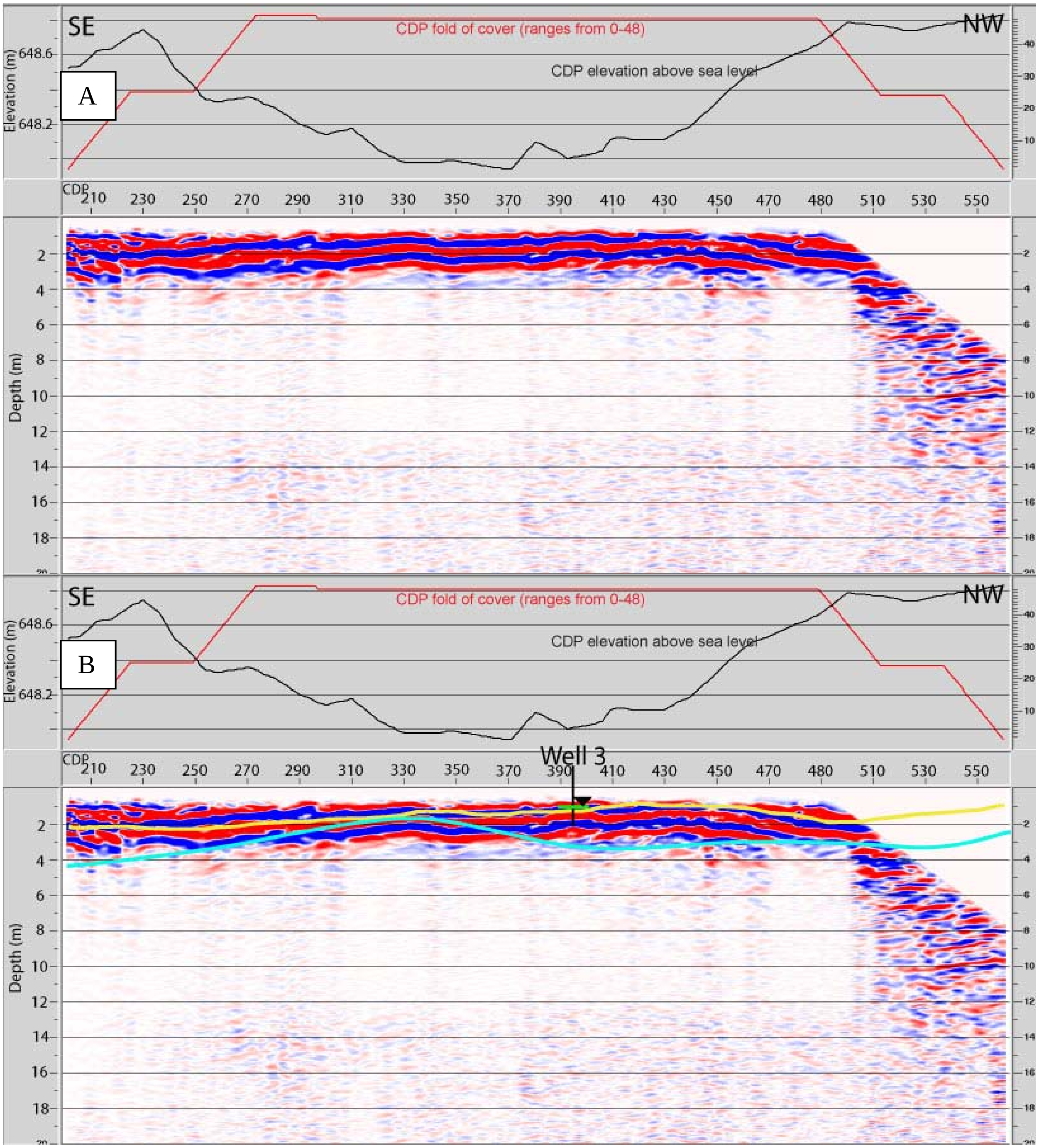

Figure 12. A) Seismic profile 1 at Carson Slough site. Source and receiver spacing is 1 ft (0.3047 m) and CDP spacing is 0.5 ft (0.1524 m).
B) Seismic profile for Carson Slough profile 1 with location of wells 4 and its corresponding measured depth to water marked by green line with triangle. EM interpretation is of depth to water are marked by the light blue line with satation 13 on the left to station 9 on the right. Yellow line represents depth to first rigid layer determined by refraction models from the shot records.

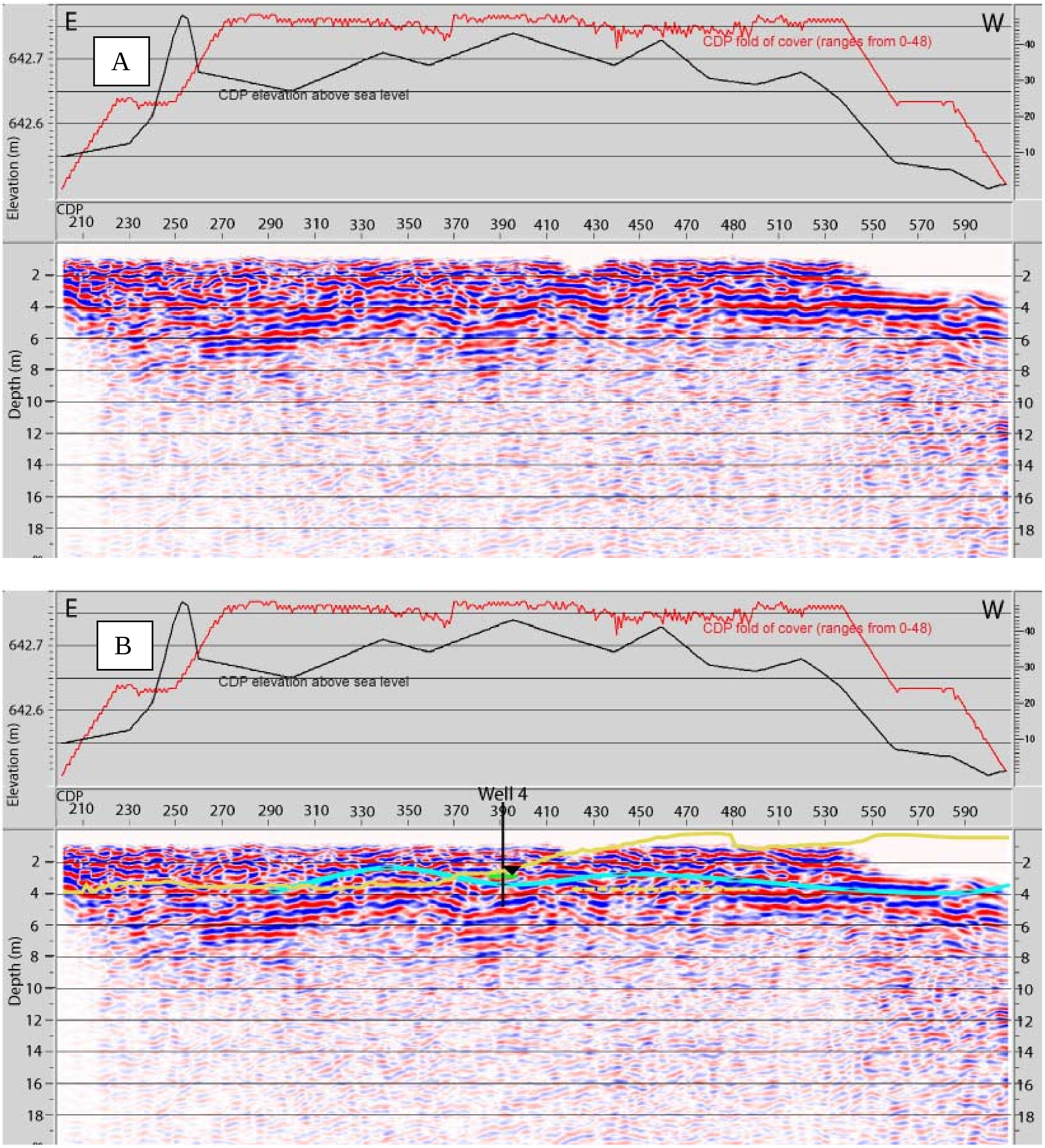

Figure 13. A) Stacked section for Carson Slough profile 2. Source and receiver spacing is 1 ft (0.3047 m) and CDP spacing is 0.5 ft (0.1524 m).
B) Seismic profile for Carson Slough profile 2 with location of wells 4 and its corresponding measured depth to water marked by green line with triangle. EM interpretation is of depth to water are marked by the light blue line with satation 1 on the left to station 7 on the right. Yellow line represents depth to first rigid layer determined by refraction models from the shot records. Dashed yellow line represents a possible second rigid layer.

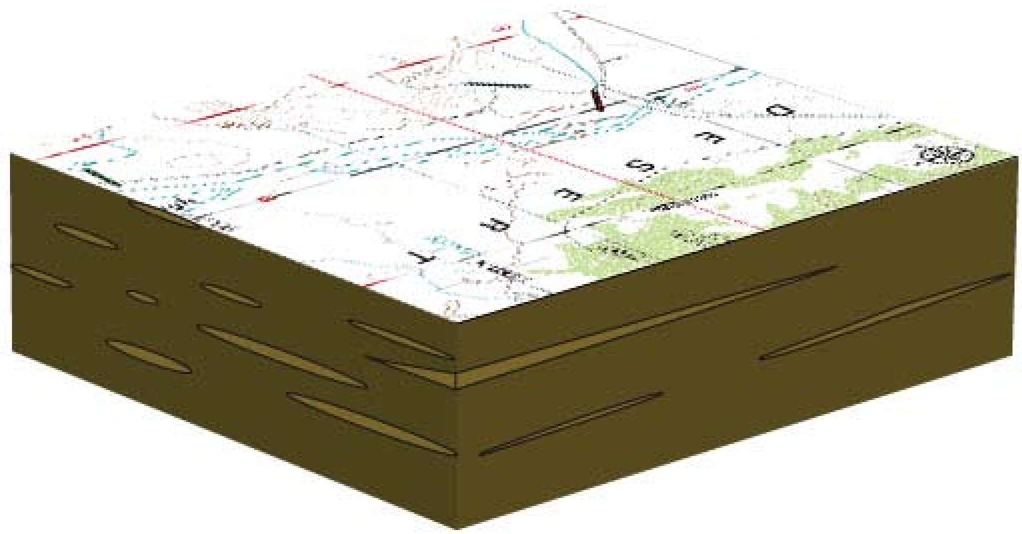

Figure 14. Interpretation of Carson Slough subsurface composed of fine grained channels surrounded by a matrix of clays and other fine grain sediments and sands, with a topographic map from Figure 1-B of the Carson Slough area on top.

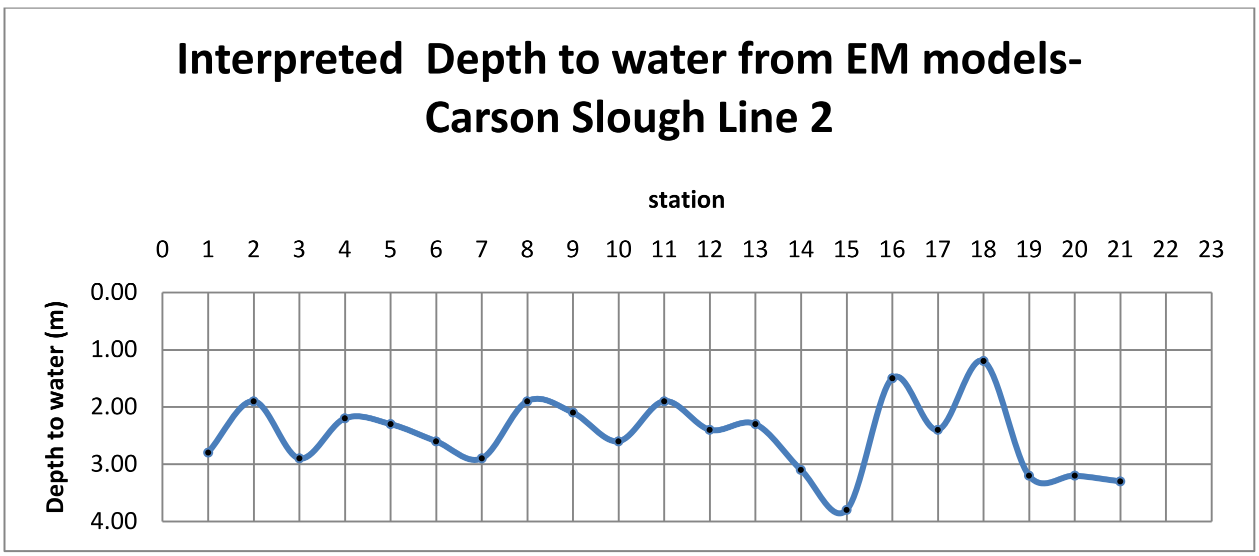

Figure 15. Depth to water using an interpretation where depth to water is at the point immediately below the conductivity peak for Line 2 at Carson Slough. Interpreted using individually modeled station (as opposed to modeling as a profile). Each station is 10 m apart

TABLES

Table 1. AA results for soil samples from Palmyra, UT site well #1 from Na^+ concentrations from leachate at various detphs

Depth (m)	Depth (ft.)	Na+ mg/L
0.1524	0.5	7
0.4572	1.5	1034
1.3716	4.5	728
1.6764	5.5	1848
2.286	7.5	1853
2.7432	9	2122
3.2004	10.5	1661
3.5052	11.5	1653

Table 2. Data from augered holes at both the Palmyra, UT and Carson Slough, NV sites. Depth to water for the Palmyra site is to water table. Depth to water for Carson Slough wells is to potentiometric surface. Soil classification abbreviations are listed at the end.

			Palmyra well 1 USCS classification symbol	Palmyra well 2 USCS classification symbol	Carson Slough well 1 USCS classification symbol	Carson Slough well 2 USCS classification symbol
Ground elevation (ft.)					2135.4	2130.9
Depth to water			9.5	9.8	10.1	4.6
Line					line 4	line 4
Depth interval						
0.0	to	1	ML	ML	SP-SM	SP-SM
1.0	to	1.5	ML	ML	SP-SM	SP-SM
1.5	to	2	ML	ML	SP-SM	SP-SM
2.0	to	2.5	ML	ML	SP-SM	SC
2.5	to	3	ML	ML	SP-SM	SC
3.0	to	3.5	ML	ML	SP-SM	SC
3.5	to	4	ML	ML	SP-SM	SC
4.0	to	4.5	ML	ML	SC	SC
4.5	to	5	ML	ML	SC	SC
5.0	to	5.5	ML	ML	SC	CL
5.5	to	6	ML	ML	SC	CL
6.0	to	6.5	ML	ML	SC	CL
6.5	to	7	ML	ML	SC	CL
7.0	to	7.5	SM	SM	SC	CL
7.5	to	8	SM	SM	SC	CL
8.0	to	8.5	ML	ML	SC	CL
8.5	to	9	ML	ML	SC	CL
9.0	to	9.5	ML	ML	CL	
9.5	to	10	ML	ML	CL	
10.0	to	10.5	ML	ML	CL	
10.5	to	11	ML	ML	CL	
11.0	to	11.5	ML	ML	CL	
11.5	to	12	ML	ML	CL	
12.0	to	12.5			CL	
12.5	to	13			CL	

	Carson Slough well 3 USCS classification symbol	Carson Slough well 4 USCS classification symbol	Carson Slough well 5 USCS classification symbol	Carson Slough well 6 USCS classification symbol
Ground elevation (ft.)	2126.0	2108.7	2107.4	2108.3
Depth to water	3.1	9.2	6.4	4.5
Line	line 1	line 2	line 2	line 2
Depth interval				
0.0 to 1	SM	CL	SM	CL
1.0 to 1.5	SM	GC	SM	CL
1.5 to 2	SM	GC	SM	CL
2.0 to 2.5	SM	SC	SM	ML
2.5 to 3	SM	SC	SM	ML
3.0 to 3.5	SP-SM	SC	ML	ML
3.5 to 4	SP-SM	SC	ML	ML
4.0 to 4.5	SP-SM	SC	ML	ML
4.5 to 5	CL	SC	ML	ML
5.0 to 5.5	CL	SC	ML	CL
5.5 to 6	CL	SC	ML	CL
6.0 to 6.5	CL	SC	SP	CL
6.5 to 7	CL	GC	SM	CL
7.0 to 7.5	SC	CL	SM	CL
7.5 to 8	SC	CL	SM	CL
8.0 to 8.5	SC	CL	SM	CL
8.5 to 9	SC	CL	SM	caliche
9.0 to 9.5	CL	CL	CL	
9.5 to 10	CL	CL	CL	
10.0 to 10.5	CL	CL		
10.5 to 11	CL	CL		
11.0 to 11.5	CL	CL		
11.5 to 12	CL	CL		
12.0 to 12.5	CL	CL		
12.5 to 13	CL	CL		
13.0 to 13.5		CL		
13.5 to 14		CL		
14.0 to 14.5		CL		
14.5 to 15		CL		

				Carson Slough well 7 USCS classification symbol	Carson Slough well 8 USCS classification symbol	Carson Slough well 9 USCS classification symbol
Ground elevation (ft.)				2096.0	2096.8	2095.8
Depth to water				15.4	7.8	5.7
Line				not on a line	line 3	line 3
Depth interval						
0.0	to	1		SW-SC	SC	SW-SC
1.0	to	1.5		SW-SC	SC	SW-SC
1.5	to	2		SW-SC	SC	SW-SC
2.0	to	2.5		SW-SC	SC	CL
2.5	to	3		SW-SC	SC	CL
3.0	to	3.5		SW-SC	SC	CL
3.5	to	4		SW-SC	SC	CL
4.0	to	4.5		SW-SC	CL	SW-SC
4.5	to	5		SW-SC	CL	SW-SC
5.0	to	5.5		SW-SM	CL	SC
5.5	to	6		SW-SM	CL	SC
6.0	to	6.5		SW-SM	CL	SC
6.5	to	7		SW-SM	CL	SC
7.0	to	7.5		CL	CL	SW
7.5	to	8		CL	CL	SW
8.0	to	8.5		CL	CL	
8.5	to	9		CL	CL	
9.0	to	9.5		CL	CL	
9.5	to	10		CL	CL	
10.0	to	10.5		CL	CL	
10.5	to	11		CL	CL	
11.0	to	11.5		CL	CL	
11.5	to	12		CL	CL	
12.0	to	12.5		CL	CL	
12.5	to	13		CL	CL	
13.0	to	13.5		CL		
13.5	to	14		CL		
14.0	to	14.5		CL		
14.5	to	15		CL		
15.0	to	15.5		CL		
15.5	to	16		CL		

CL= Clay; GC= Clayey Gravel; ML= Silt; SC= Clayey Sand;
SM= Silty Sand; SP= Poorly Graded Sand; SW= Well Graded Sand

Table 3. Data for wells 1-9 in the Carson Slough, Nevada area (CS) plus an additional borehole (BH) and wells 1-2 at Palmyra, Utah (P). All data is from August 31, 2007 except for the last two rows which are from Sept. 25, 2007 and and the two columns for Palmyra, UT wells which are from October, 2008.

ID	CS well 1	CS well 2	CS well 3	CS well 4	CS well 5	CS well 6
Aug. 31, 2007						
UTM easting	556534.80	556599.00	556947.94	556410.33	556489.25	556563.32
UTM northing	4029705.66	4029758.00	4029877.22	4028259.80	4028250.98	4028236.22
Well Depth (ft.)	13.5	9.74	13.21	18.80	11.14	9.90
Temperature C	23.8	25.2	25.8	21.6	26.4	no data
pH	7.83	7.82	8.04	7.86	7.63	no data
Conductivity mS/m	84.8	234	396	619	627	no data
Water Elevation (ft)	2125.27	2126.32	2122.85	2099.48	2100.95	2103.73
Depth to Water (ft.)	10.1	4.6	3.1	9.2	6.4	4.5
Depth to Water (m)	3.08	1.41	0.96	2.82	1.96	1.38
Pressure Head	no data	1.50	no data	0.00	1.00	0.00
Sept. 25, 2007						
Water depth (ft.)	10.6	5.05	no data	8.14	5.97	7.22
Change in Water elevation (ft.)	-0.49	-0.44	no data	1.10	0.45	-2.68

ID	CS well 7	CS well 8	CS well 9	CS BH-1	P well 1	P well 2
Aug. 31, 2007						
UTM easting	556068.97	556357.50	556446.49	556422.54		
UTM northing	4027279.39	4027252.50	4027232.76	4028346.90		
Well Depth (ft.)	16.50	12.01	9.10	14.30		
Temperature C	no data	24.8	30.1	21.8		
pH	no data	8.45	7.95	8.11		
Conductivity uS/m	no data	1330	1640	381	5310	
Water Elevation (ft)	2080.62	2088.98	2090.13	2100.16		
Depth to Water (ft.)	15.4	7.8	5.7	7.6	9.4	9.7
Depth to Water (m)	4.69	2.39	1.74	2.32	2.9	3.0
Pressure Head	no data	no data	no data	4.00	0.0	0.0
Sept. 25, 2007						
Water depth (ft.)	no data	no data	no data	no data		
Change in Water Level (ft.)	no data	no data	no data	no data		

APPENDIX A

Appendix A-1. XRD RockJock analyses showing approximate mineralogy for samples from the Palmyra, UT site well #1.

Sample name:	P1 1.5	P1 4.5	P1 5.5	P1 7.5	P1 9.0	P1 10.5	P1 11.5
Full pattern degree of fit:	0.185	0.172	0.175	0.227	0.158	0.161	0.211
Mineral	Weight %	Weight %	Weight %	Weight %	Weight %	Weight %	Weight %
NON-CLAYS							
Quartz	42.2	44.8	35.2	45.3	23.9	43.2	58
Anorthoclase feldspar	8.4	8.1	11.9	17.7	7.3	10.7	13.1
Calcite	39.9	14.3	24.9	13.8	29.5	21.6	14.5
Dolomite	9.5	3.8	6.6	4.2	5.2	6	3.6
Mordenite	0	14.6	2.4	12.5	10	1.8	6.4
Total non-clays	100	85.6	81	93.6	76	83.2	95.6
CLAYS							
Na-Smectite (Wyo)	0	14.4	19	6.4	24	16.8	4.4
Total clays	0	14.4	19	6.4	24	16.8	4.4
TOTAL	100	100	100	100	100	100	100

Appendix A-2. XRD RockJock analyses showing approximate mineralogy for samples from the Carson Slough site well #4.

Sample name:	CS4 1.6	CS4 3.3	CS4 4.5	CS4 5.8	CS4 6.8	CS4 7.8	CS4 9.0	CS4 9.8	CS4 10.7	CS4 12.1
Full pattern degree of fit:	0.159	0.139	0.14	0.168	0.163	0.139	0.156	0.143	0.143	0.164
Mineral	Weight %	Weight %	Weight %	Weight %	Weight %	Weight %	Weight %	Weight %	Weight %	Weight %
NON-CLAYS										
Quartz	14.6	1.8	6.9	16.7	20.7	6.2	1.7	0.9	2.2	16.9
Sanidine feldspar	10.9	16.6	8.3	16.2	18.3	14.2	12.8	18.3	18.9	13.8
Anorthoclase feldspar	38	13.7	28.7	51.5	42.5	22.7	19.9	17	19.7	44.1
Calcite	28.9	15.5	53.9	9.5	0.7	3	1.4	2	3.8	20.7
Dolomite	1.7	24.4	1.6	0.2	0.5	36.8	44.2	39.4	27.8	1.4
Total non-clays	94.1	72	99.4	94	82.7	82.9	80	77.6	72.4	96.8
CLAYS										
Illite	5.9	28	0.6	6	17.3	17.1	20	22.4	27.6	3.2
Total clays	5.9	28	0.6	6	17.3	17.1	20	22.4	27.6	3.2
TOTAL	100	100	100	100	100	100	100	100	100	100

Appendix A-3. Raw EM conductivity data for line at Palmyra, UT and the 4 lines at Carson Slough

Instrument -->						EM-38	EM-38	EM-38	EM-38	EM-31-SH	EM-31-SH	EM-31-SH	EM-31-SH	EM-34	EM-34	EM-34	EM-34
Frequency -->						14600 Hz	14600 Hz	14600 Hz	14600 Hz	9800 Hz	9800 Hz	9800 Hz	9800 Hz	6400 Hz	6400 Hz	1600 Hz	1600 Hz
coil separation -->						1m	1m	1m	1m	2m	2m	2m	2m	10m	10m	20m	20m
Dipole oridentation -->						veritcal	horizontal	veritcal	horizontal	veritcal	horizontal	veritcal	horizontal	veritcal	horizontal	veritcal	horizontal
height above ground ->						1.0 m	1.0 m	0	0	0.95	0.95	0	0	0	0	0	0
		UTM easting Zone 11S	UTM northing zone 11S	elevation (feet)	elevation (meters)	mS/m	mS/m	mS/m	mS/m	mS/m	mS/m	mS/m	mS/m	mS/m	mS/m	mS/m	mS/m
Palmyra, UT	Station #																
	1					95	48	246	174	249	141	422	294	44	238	32	224
	(well 1) 2					88	43	221	132	247	135	407	261	38	238	45	241
	3					92	45	235	135	248	129	431	260	41	240	34	238
	4					93	45	232	142	248	135	427	270	45	233	26	226
	5					90	43	221	134	246	130	412	260	49	219	36	226
	6					87	42	213	126	229	123	391	242	50	224	45	221
	7					89	43	225	131	235	127	406	258	59	220	40	219
	(well2) 8					93	46	222	139	237	138	389	257	65	220	36	219
	9					97	47	237	142	254	138	438	278	37	236	25	221
	10					114	57	300	213	291	162	480	351	35	240	13	233
Carson Slough	Station #																
Line 1	1	556866.8	4029935.08	2130.16	649.2741	58	28	190	129	127	71	205	176	48	134	63	146
Line 1	2	556874.83	4029929.34	2129.3	649.0119	53	27	163	121	125	71	203	169	71	133	64	144
Line 1	3	556883.01	4029923.59	2129.97	649.2162	55	28	182	123	126	77	226	184	34	135	64	135
Line 1	4	556891.09	4029917.73	2129.28	649.0058	33	15	82	54	91	47	143	90	82	116	66	135
Line 1	5	556899.15	4029911.9	2129.55	649.0881	46	23	147	118	103	65	147	153	57	120	93	128
Line 1	6	556907.32	4029906.18	2129.41	649.0455	51	26	161	134	118	67	167	160	65	120	72	136
Line 1	7	556915.41	4029900.39	2129.27	649.0028	58	29	189	161	132	79	200	192	49	123	55	137
Line 1	8	556923.56	4029894.57	2128.79	648.8565	57	30	174	159	134	79	187	206	70	119	80	141
Line 1	9	556931.79	4029888.82	2128.46	648.7559	67	34	232	199	142	91	194	227	52	124	71	139
Line 1	10	556939.9	4029883.17	2127.55	648.4785	62	31	194	156	143	83	223	205	51	135	62	142
Line 1	(Well 3) 11	556947.94	4029877.22	2125.99	648.0031	59	31	135	175	135	84	160	198	76	137	84	148
Line 1	12	556956.05	4029871.44	2125.93	647.9848	68	36	200	223	144	92	146	243	92	139	88	157
Line 1	13	556964.22	4029865.61	2127	648.3109	72	37	213	182	168	97	261	233	54	156	50	164
Line 1	14	556972.36	4029859.84	2127.66	648.5121	88	46	296	221	206	119	313	292	48	182	30	177
Line 1	15	556980.5	4029854.08	2128.47	648.759	84	44	270	217	206	127	335	316	35	199	38	188
Line 1	16	556988.61	4029848.17	2127.76	648.5426	99	51	331	264	234	137	357	354	59	190	52	190
Line 1	17	556996.75	4029842.47	2128.83	648.8687	75	38	206	137	193	109	326	242	48	190	48	198
Line 1	18	557004.87	4029836.66	2128.61	648.8016	89	45	276	173	240	133	422	291	37	216	14	216

Line 1	19	557013.1	4029830.86	2127.6	648.4938	134	67	408	301	327	181	532	455	5	245	5	232
Line 1	20	557021.18	4029825.08	2127.28	648.3962	141	74	487	387	332	200	520	522	13	250	17	244
Line 1	21	557029.34	4029819.39	2127.1	648.3414	167	87	592	507	374	230	589	634	0	252	50	244
Line 2	1	556390.51	4028262.15	2108.47	642.6629	85	43	279	192	218	129	361	307	33	206	49	203
Line 2	2	556400.39	4028260.92	2108.56	642.6904	83	39	275	141	220	119	440	267	57	202	26	182
Line 2	(well 4) 3	556410.33	4028259.8	2108.72	642.7391	63	31	186	129	164	99	274	229	81	172	83	162
Line 2	4	556420.23	4028258.58	2108.68	642.727	51	23	135	78	142	75	238	148	129	127	72	151
Line 2	5	556430.15	4028257.46	2108.56	642.6904	52	23	138	80	141	77	237	158	117	137	105	151
Line 2	6	556440.1	4028256.5	2108.01	642.5227	75	38	249	158	185	109	329	252	64	173	66	160
Line 2	7	556450.01	4028255.52	2107.9	642.4892	111	59	410	363	249	153	351	415	33	184	52	164
Line 2	8	556459.93	4028254.45	2108.2	642.5807	89	44	298	205	215	122	358	290	72	183	48	166
Line 2	9	556469.8	4028253.09	2108.4	642.6416	71	36	222	177	170	104	264	243	85	163	64	157
Line 2	10	556479.78	4028252	2108.07	642.541	55	27	169	112	141	82	234	176	70	148	73	154
Line 2	(well 5) 11	556489.25	4028250.98	2107.37	642.3277	48	22	136	80	126	68	221	149	78	135	79	152
Line 2	12	556499.56	4028249.85	2107.87	642.4801	37	17	100	56	108	58	185	114	82	132	76	150
Line 2	13	556509.47	4028248.82	2108.38	642.6355	34	17	88	58	96	55	152	108	122	127	103	150
Line 2	14	556519.45	4028247.81	2110.17	643.1811	43	21	99	59	111	61	175	117	67	130	110	149
Line 2	15	556529.34	4028246.54	2109.68	643.0318	73	36	226	156	175	100	300	242	38	160	46	152
Line 2	16	556539.26	4028245.41	2108.26	642.5989	93	50	264	281	218	130	295	316	68	198	50	159
Line 2	17	556549.09	4028244.33	2108.75	642.7483	68	34	208	150	162	92	255	203	108	161	88	165
Line 2	18	556559.05	4028243.31	2108.28	642.605	68	34	208	150	162	92	255	203	108	161	88	165
Line 2	19	556568.98	4028242.13	2108.33	642.6203	74	38	223	154	187	102	321	233	61	176	76	159
Line 2	20	556578.81	4028241.02	2109.34	642.9281	64	33	197	132	162	95	272	210	49	177	75	157
Line 2	21	556588.74	4028239.72	2110.06	643.1476	51	25	143	92	131	75	224	164	65	159	69	151
Line 3	1	556259.98	4027274.43	2098.33	639.5723	78	40	249	143	214	115	385	250	56	203	46	202
Line 3	2	556269.73	4027272.19	2098.27	639.554	80	38	224	138	213	112	373	239	38	199	58	203
Line 3	3	556279.48	4027269.99	2098.66	639.6729	72	38	205	126	193	111	340	242	69	209	41	197
Line 3	4	556289.26	4027267.81	2098.43	639.6027	70	33	167	103	190	101	333	196	59	180	40	191
Line 3	5	556299	4027265.67	2097.98	639.4656	62	31	159	94	169	90	285	184	73	177	54	181
Line 3	6	556308.77	4027263.5	2097.13	639.2065	46	23	108	64	128	72	213	133	76	165	81	179
Line 3	7	556318.57	4027261.24	2097.02	639.173	44	21	105	62	127	67	205	123	76	155	86	176
Line 3	8	556328.34	4027259.18	2097.45	639.304	46	22	115	67	129	70	214	130	67	158	65	182
Line 3	9	556337.94	4027256.87	2097.07	639.1882	53	26	133	80	145	82	244	154	88	176	88	185
Line 3	10	556347.71	4027254.73	2097.37	639.2797	54	26	119	72	149	83	235	148	57	184	70	192
Line 3	(well 8) 11	556357.5	4027252.5	2096.83	639.1151	78	39	229	145	204	112	324	247	79	189	76	195
Line 3	12	556367.29	4027250.26	2097.36	639.2766	89	45	269	174	230	128	393	288	43	197	29	199
Line 3	13	556376.99	4027247.97	2097.76	639.3985	71	36	208	132	187	102	317	220	68	196	49	203

Line 3	14	556386.74	4027245.78	2097.42	639.2949	66	33	173	109	174	97	298	201	80	186	63	200
Line 3	15	556396.55	4027243.66	2097.57	639.3406	82	41	251	158	209	118	355	272	30	190	63	196
Line 3	16	556406.34	4027241.61	2096.83	639.1151	80	41	226	174	201	121	323	266	96	198	46	199
Line 3	17	556416.02	4027239.5	2097.51	639.3223	68	35	195	130	179	103	285	218	59	189	39	196
Line 3	18	556425.88	4027237.33	2098.02	639.4778	52	27	136	84	141	78	236	164	78	175	72	187
Line 3	19	556435.54	4027235.21	2097.64	639.362	55	27	141	81	145	78	244	148	81	163	68	194
Line 3	20	556445.36	4027233.09	2095.98	638.856	76	36	219	164	185	111	292	255	75	174	85	177
Line 3	well 9	556446.49	4027232.76	2095.84	638.8133												
Line 3	21	556454.84	4027230.91	2099.63	639.9685	35	17	76	38	105	57	172	98	101	166	35	200
Line 4	1	556519.26	4029693.12	2137.22	651.426	39	14	100	84	84	51	124	119	80	96	72	90
Line 4	2	556526.95	4029699.45	2136.65	651.2522	36	14	96	68	81	51	125	107	78	104	58	96
Line 4	(well 1) 3	556534.8	4029705.66	2135.38	650.8651	47	19	143	101	104	62	169	149	50	106	60	97
Line 4	4	556542.53	4029712.04	2134.62	650.6335	47	19	132	95	101	60	151	142	71	109	59	97
Line 4	5	556550.28	4029718.31	2134.05	650.4597	43	16	112	66	97	53	170	115	61	106	56	97
Line 4	6	556557.96	4029724.57	2133.23	650.2098	45	18	121	93	92	59	138	135	69	109	69	93
Line 4	7	556565.65	4029730.93	2132.68	650.0422	41	15	104	73	91	51	132	115	86	102	78	99
Line 4	8	556573.55	4029737.22	2132.09	649.8623	46	17	109	74	101	60	159	133	64	109	62	100
Line 4	9	556581.12	4029743.5	2131.84	649.7861	43	15	107	64	99	56	158	120	62	117	64	109
Line 4	10	556588.84	4029749.61	2131.47	649.6734	40	15	92	59	89	48	135	104	87	114	70	113
Line 4	11	556596.61	4029756.07	2131.17	649.5819	44	17	99	70	101	53	145	112	89	119	82	120
Line 4	well 2	556599	4029758	2130.93	649.5088	44	21	131	102	112	64	172	141	90	117	85	119
Line 4	12	556604.41	4029762.39	2130.35	649.332	66	28	182	172	141	82	203	211	74	140	66	119
Line 4	13	556612.09	4029768.77	2130.34	649.3289	73	31	216	158	164	89	266	220	48	148	46	124
Line 4	14	556619.81	4029774.93	2130.31	649.3198	56	25	144	134	119	74	168	185	94	137	70	120
Line 4	15	556627.62	4029781.24	2131.26	649.6094	36	11	75	45	83	42	137	92	86	112	82	118
Line 4	16	556635.44	4029787.56	2130.98	649.524	32	10	68	41	76	37	115	84	86	100	82	111
Line 4	17	556643.11	4029793.88	2130.51	649.3808	35	12	85	55	81	41	125	96	74	100	80	107
Line 4	18	556650.86	4029800.08	2130.66	649.4265	37	13	88	51	83	45	135	99	70	102	86	107
Line 4	19	556658.58	4029806.49	2130.74	649.4509	34	11	83	55	76	42	123	95	83	101	81	108
Line 4	20	556666.3	4029812.78	2130.91	649.5027	36	12	89	57	79	40	133	96	64	102	72	107
Line 4	21	556674	4029818.99	2131.47	649.6734	35	11	75	49	75	44	120	88	67	99	67	109

Appendix A-4. Carson Slough FEM 2D profiles

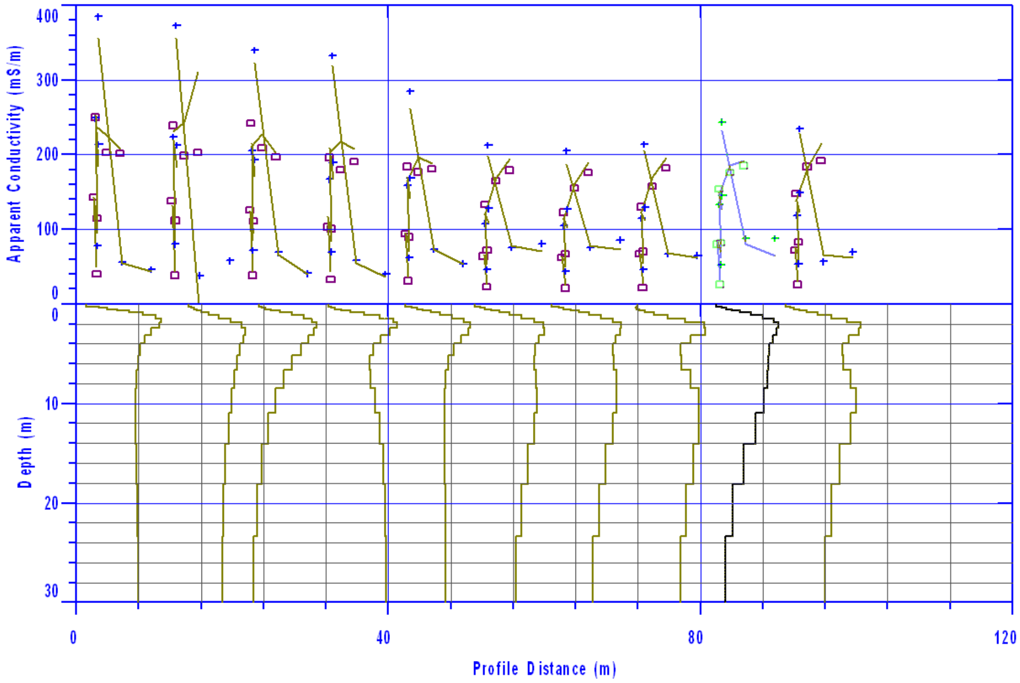

Line 3 stations 1-10 from right to left.

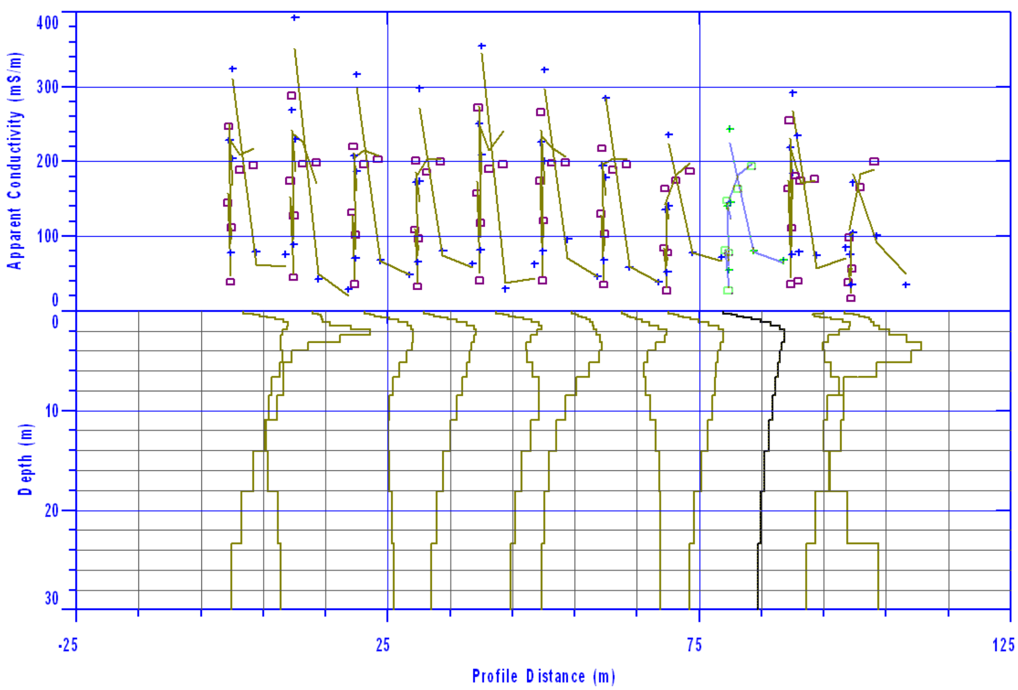

Line 3 Stations 11-21 from right to left.

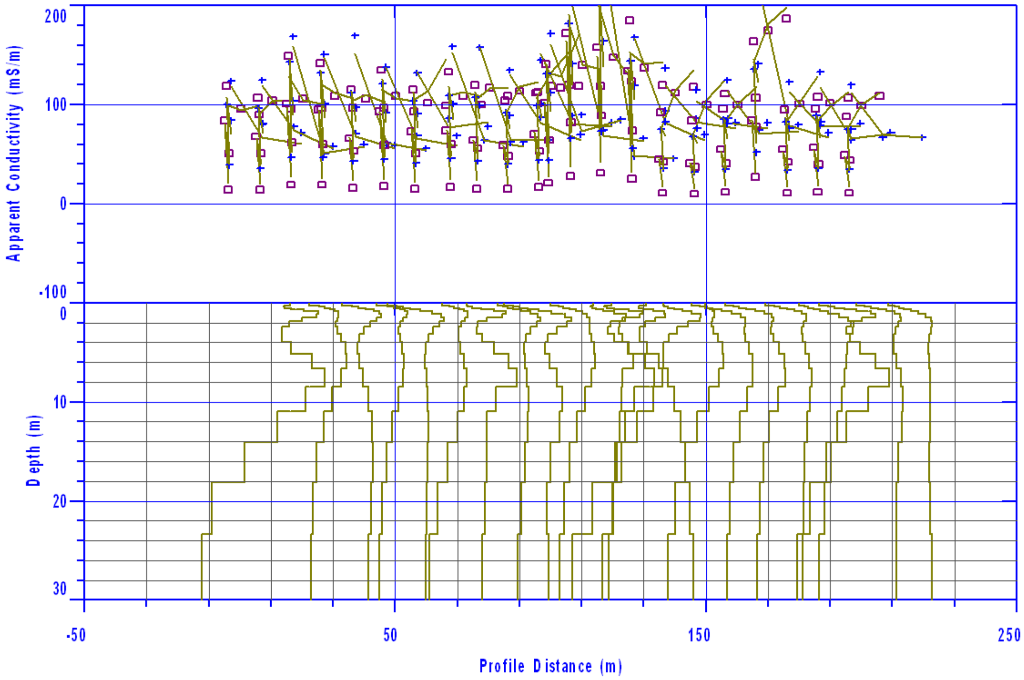

Line 4. Stations 1-21 from left to right.